

SYNTHESIS AND CHARACTERIZATION OF TRANSITION METAL OXIDES

A DISSERTATION

*Submitted in partial fulfillment of the
requirements for the award of the degree*

of

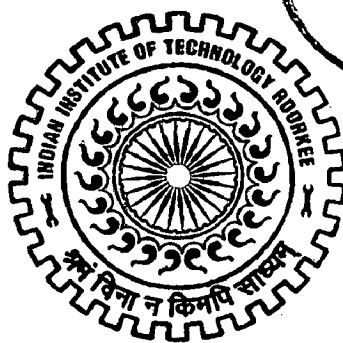
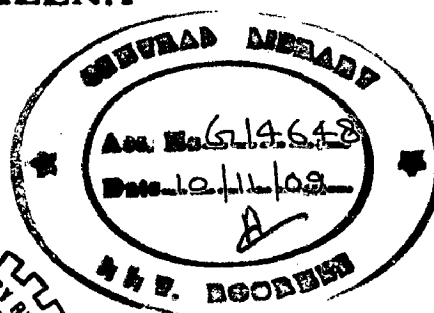
MASTER OF TECHNOLOGY

in

ADVANCED CHEMICAL ANALYSIS

By

JAY SINGH MEENA



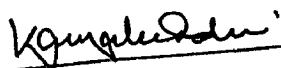
DEPARTMENT OF CHEMISTRY
INDIAN INSTITUTE OF TECHNOLOGY ROORKEE
ROORKEE-247 667 (INDIA)

JUNE, 2009

10

CERTIFICATE

It is certified that the Dissertation report entitled "SYNTHESIS AND CHARACTERIZATION OF TRANSITION METAL OXIDES" is the result of work carried out during the period of 1st July, 2008 to 30th June, 2009, by Jay Singh Meena, Department of Chemistry, Indian Institute of Technology Roorkee, under my supervision. His work neither in part nor in whole has been submitted for any other degree.



Dr. Kamaluddin,

Professor and Head

Department of Chemistry

IIT Roorkee -247 667

Date: 30/6/09

Place: Roorkee



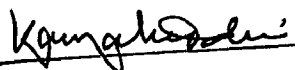
Jay Singh Meena

M.Tech. (IInd year)

CANDIDATE'S DECLARATION

I hereby declare that the work which is being presented in the project entitled "SYNTHESIS AND CHARACTERIZATION OF TRANSITION METAL OXIDES" in partial fulfillment of the requirements for the award of the degree of Masters of Technology submitted in the Department of Chemistry, IIT Roorkee is an authentic record of my own work carried out during the period from July, 2008 to June, 2009 under the supervision and guidance of Prof. Kamaluddin.

The matter embodied in this project work has not been submitted for the award of any other degree.



Dr. Kamaluddin,

Professor and Head

Department of Chemistry

IIT Roorkee -247 667

Date : 30/6/09

Place: Roorkee



Jay Singh Meena

M.Tech. (IInd)

ACKNOWLEDGEMENT

During my tenure of work at Indian Institute of Technology (IITR), in the period of July, 2008-June, 2009 as a part of my Dissertation work, I met many diligent people who have been my source of inspiration.

I would like to take this opportunity to express my heartiest sense of gratitude to my guide, Dr. Kamaluddin, Professor and Head of Chemistry Department, IIT Roorkee. I am also equally thankful to Dr. Tokeer Ahmed, Lecturer, Department of Chemistry, Jamia Millia Islamia (Central University), Delhi for his inspiration during the entire period of my project work.

I am much beholden to my colleagues Mr. Uma Shankar (SRF), Mr. Brij Bhushan (JRF) and Mr. Anand Kumar (JRF) for their assistance and suggestions throughout the Dissertation work.

I am extremely thankful to 'The Head of the Institute Instrumentation Centre', IIT Roorkee for providing instrumentation facilities to carry out my project work.

I would like to express my sincere thanks to Prof. R. N. Goyal, Prof. U. P. Singh, Prof. M.R. Maurya, Dr. P. P. Thankachan, Dr. R. K. Dutta, Dr. K. R. Justin Thomas, Dr. R.K. Peddinti, Dr. P. Jeevanandan, and all faculty member of chemistry department for their support during my M.Tech. Degree.

A special thanks to Dr. Vivek Acharya, Earth Science and Mr. Mukesh Kumar, Research Scholar, Institute Instrumentation Centre, IIT Roorkee for his support throughout.

I would like to thank my friends Abhishek Baheti, Satya prakash Singh, Rajiv Sachdeva, Goverdhan, Shriom Singh, and Rituraj Dubey for their perennial support. Their interest in my work has been a moral booster, enabling me to perform even better.

Finally I would like to thank my beloved parents and family members whose blessing and enthusiastic efforts have always been a continuous source of inspiration to engage myself in higher pursuits.

Date:

Roorkee

Jay Singh Meena

M.Tech II Year

ABSTRACT

Owing to the large specific surface area and other superior properties over their bulk counterparts arising from quantum size effect, nanoscaled and nanostructured materials have attracted considerable research interest. Many novel nanoscale materials have been synthesized in the past 10 years. It is well known that the behaviors of nanomaterials strongly depend on the sizes, shape, dimensionality and morphologies, which are thus the key factors to their ultimate performance and applications. Therefore, it is of great interest to synthesize nanomaterials with a controlled structure and morphology.

Manganese, cobalt and zinc oxides are important materials due to their wide applications in the area of catalysis, magnetic material and electrode material for batteries. These oxides were prepared by calcinations of their respective hydroxides under specific conditions. Manganese, Cobalt, and Zinc hydroxides in turn were prepared from liquid ammonia and their nitrate salts by the precipitation method. Their characterization was done using TGA/DTA, XRD, SEM and SQUID.

TGA studies of manganese oxide (Mn_2O_3) suggested that it existed in hydrated form at low temperature and converted to anhydrous manganese oxide at around $650^{\circ}C$. While Cobalt and Zinc hydroxides existed in hydrated form at low temperatures and converted to anhydrous oxides at around $200^{\circ}C$ and $150^{\circ}C$ respectively. XRD studies suggested that their oxides have different Size with different form of oxides in different atmosphere. The particle size as calculated from the XRD data using the Sherrere Formula suggested that the particles were in nano-range. The Particle size, in different atmosphere, determined was in the range 16-76nm, 1-46nm and 23-43nm for the manganese oxides, cobalt oxides and zinc oxides, respectively. The results obtained from SEM and SQUID were also in good agreement with XRD results.

CONTENTS

Certificate	i
Candidate's Declaration	iii
Acknowledgement	v
Abstract	vii
Content	ix

CHAPTER -1 INTRODUCTION

- 1.1. Metal Oxides
- 1.2. Preparation of metal oxides
 - 1.2.1. Ceramic method
 - 1.2.2. Precursor method
 - 1.2.3. Topochemical reactions
 - 1.2.4. Intercalation Method
 - 1.2.5. Sol- Gel Synthesis
 - 1.2.6. High – Pressure Synthesis
 - 1.2.7. Ion Exchange Method
 - 1.2.8. Alkali Flux and Electrochemical Method
 - 1.2.9. Crystal Growth Method
- 1.3. Magnetic Properties of metal oxides
- 1.4. Application of metal oxides
 - 1.4.1. Catalyst
 - 1.4.2. Superconductor
 - 1.4.3. Adsorbent
 - 1.4.4. Sensor
 - 1.4.5. Electrode
- 1.5. Manganese
 - 1.5.1. Isotopes
 - 1.5.2. Physical Properties
 - 1.5.3. Physiological Properties
 - 1.5.4. Chemical Properties
 - 1.5.5. Manganese in compounds
 - 1.5.6. Different forms of manganese oxides
 - 1.5.6.1. Manganese Monoxide
 - 1.5.6.2. Diamanganese Trioxide
 - 1.5.6.3. Manganese Dioxide
 - 1.5.7 Application of Manganese Oxide

1.6. Cobalt

- 1.6.1. Isotopes
- 1.6.2. Occurrence
- 1.6.3. Compounds
- 1.6.4. Cobalt oxides
- 1.6.5. Chalcogen compounds
- 1.6.6. Application of cobalt oxides

1.7 Zinc

- 1.7.1 Isotopes
- 1.7.2 Compounds
- 1.7.3 Electrochemistry
- 1.7.4 Zinc oxide
- 1.7.5 Chemical properties
- 1.7.6 Crystal structure
- 1.7.7 Mechanical properties
- 1.7.8 Electronic properties
- 1.7.9 Application of zinc oxides
 - 1.7.9.1 Chemical and biosensor applications
 - 1.7.9.2 Use in semiconductors
 - 1.7.9.3 Cigarette filters
 - 1.7.9.4 Zinc oxide nanorod sensor

CHAPTER – 2- EXPERIMENTAL

2.1 Materials Used

2.2 Equipments Used

- 2.2.1 Thermo Gravimetric Analysis – Differential Thermal Analysis
- 2.2.2 Powder X- Ray Diffraction
- 2.2.3 Field Emission-Scanning Electron Microscopy
- 2.2.4 SQUID

2.3 Synthesis of Manganese Oxide

2.4 Synthesis of Cobalt Oxide

2.5 Synthesis of Zinc Oxide

CHAPTER – 3- RESULT AND DISCUSSION

3.1 Thermo Gravimetric Analysis – Differential Thermal Analysis

3.2 X- Ray Diffraction

- 3.2.1 X-Ray Diffraction analysis of manganese oxides
- 3.2.2 X-RAY DIFFRACTION ANALYSIS OF COBALT OXIDES
- 3.2.3 X-RAY DIFFRACTION ANALYSIS OF ZINC OXIDES

3.3 SQUID

3.4 FE-SEM IMAGES AND EDAX DATA

CHAPTER – 4 – CONCLUSION

List of Tables

- Table 1: The different types of metal oxides.
- Table 2: Magnetic properties of metal oxides
- Table 3: different forms of manganese oxides with examples:
- Table 4: Weight loss for Manganese Oxides Precursor (From TGA data)
- Table 5: Weight loss for Cobalt Oxides Precursor (From TGA data)
- Table 6: Weight loss for Zinc Oxides Precursor (From TGA data)
- Table 7: X-Ray Diffraction data for Manganese Oxide (Mn_3O_4)
- Table 8: X-Ray Diffraction data for Manganese oxide (Air/ 180°C)
- Table 9: X-Ray Diffraction data for Manganese oxide (Air/ 650°C)
- Table 10: X-Ray Diffraction data for Manganese oxide (Air/ 1000°C)
- Table 11: X-Ray Diffraction data for Manganese oxide (N_2 / 450°C)
- Table 12: X-Ray Diffraction data for Manganese oxide (Ar/ 650°C)
- Table 13: X-Ray Diffraction data for Cobalt Hydroxide
- Table 14: X-Ray Diffraction data for cobalt hydroxide (Air/ 450°C)
- Table 15: X-Ray Diffraction data for cobalt hydroxide (Air/ 950°C)
- Table 16: X-Ray Diffraction data for cobalt hydroxide (Ar/ 650°C)
- Table 17: X-Ray Diffraction data for Zinc Hydroxide
- Table 18: X-Ray Diffraction data for Zinc Precursor (Air/ 200°C)
- Table 19: X-Ray Diffraction data for Zinc Precursor (Air/ 450°C)
- Table 20: X-Ray Diffraction data for Zinc Precursor (Air/ 950°C)
- Table 21: Particle size as calculated from Scherrer Formula

List of Figures

- Fig.1 TGA-DTA graph for Manganese oxide precursor
- Fig.2 TGA-DTA graph of cobalt oxide precursor
- Fig. 3 TGA-DTA graph for zinc oxide precursor
- Fig. 4 XRD graph for Manganese oxide precursor at room temperature.
- Fig. 5 XRD graph for Manganese oxide at 180⁰C temperature in presence of air.
- Fig. 6 XRD graph for Manganese oxide at 650⁰C temperature in presence of air.
- Fig. 7 XRD graph for Manganese oxide at 1000⁰C temperature in presence of air.
- Fig. 8 XRD graph for Manganese oxide at 450⁰C temperature in nitrogen environment
- Fig. 9 XRD graph for Manganese oxide at 650⁰C temperature in Argon environment.
- Fig. 10 Magnetization graph of Mn₃O₄ at 450⁰C temperature in nitrogen environment
- Fig. 11 Magnetization graph of Mn₃O₄ at 650⁰C temperature in nitrogen environment
- Fig. 12 XRD graph for Cobalt oxide precursor at room temperature.
- Fig. 13 XRD graph for Cobalt oxide precursor at 200⁰C temperature in presence of air.
- Fig. 14 XRD graph for Cobalt oxide precursor at 450⁰C temperature in presence of air.
- Fig. 15 XRD graph for Cobalt oxide precursor at 950⁰C temperature in presence of air.
- Fig. 16 XRD graph for Cobalt oxide precursor at 450⁰C temperature in presence of nitrogen.
- Fig.17 XRD graph for Cobalt oxide precursor at 450⁰C temperature in presence of Argon
- Fig. 18 XRD graph for Zinc oxide precursor.
- Fig.19 XRD graph for Zinc oxide at 200⁰C in presence of air.
- Fig.20 XRD graph for Zinc oxide at 450⁰C in presence of air.
- Fig.21 XRD graph for Zinc oxide at 950⁰C in presence of air
- Fig. 22 SEM image & EDAX data of cobalt oxide at 200⁰C in presence of air.
- Fig. 23 SEM image & EDAX data of cobalt oxide at 450⁰C in presence of air.
- Fig. 24 SEM image & EDAX data of cobalt oxide at 950⁰C in air.
- Fig. 25 SEM image & EDAX data of zinc oxide at 200⁰C in air.
- Fig. 26 SEM image & EDAX data of zinc oxide at 450⁰C in air
- Fig. 27 SEM image & EDAX data of zinc oxide at 950⁰C in air

CHAPTER-1

INTRODUCTION AND LITERATURE REVIEW

1.1 METAL OXIDES

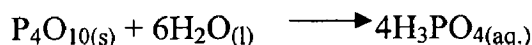
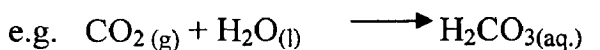
Metal oxides constitute an important class of inorganic materials which are widely applied and have many different varieties. For example, zinc oxide sintered together with other metal oxide additives have been made into non linear resistor which are called varistors for surge suppressing function. The suppressing function has been applied for switching and for random voltage protections. The corundum structure is adopted by the oxides of titanium, vanadium, chromium, iron and gallium in their +3 oxidation states as well by alumina.

Transition metals form a wide variety of oxides. Metal oxides are protected from further oxidation by forming a hard scale of oxides when it is oxidized. Not all metal oxides form a scale. If the metal oxide per mole of metal is greater than the molar volume of metal, the oxide will form a protective scale. Iron oxide and other metal oxides are used in thermite reactions, and this has been applied in many ways, including welding in spaceship repairs. Iron oxides are also the raw material for all magnets and magnetic materials used for computer disks and recording tapes [1].

Metal oxides that dissolve in water react with water to form basic solutions.



Whereas, nonmetal oxides react with water to form acidic solutions.

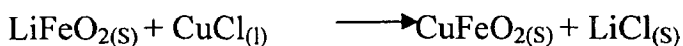
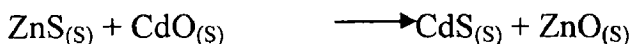
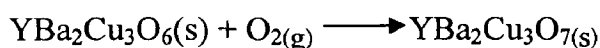


1.2 PREPARATION OF METAL-OXIDES

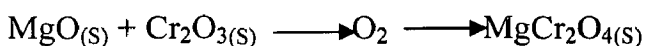
Many oxides can be directly prepared as most elements do react with oxygen at appropriate temperature and pressure conditions. Most metal in massive form react with oxygen only slowly at room temperatures because the first thin oxide coat formed protects the metal. The oxides of the alkali and alkaline-earth metals, except for beryllium and magnesium, are porous when formed on the metal surface, and they provide only limited protection to the continuation of oxidation, even at room temperatures. Gold is exceptional in its resistance to oxygen, and its oxide (Au_2O_3) must be prepared by indirect means. Noble metals react at high temperatures to form gaseous oxides although ordinarily they are resistant to oxygen.

Co-precipitation and Precursor method are commonly used methods for synthesis of oxides apart these ion exchange and alkali flux method, sol-gel method, topochemical method, electrochemical method, high pressure method (Including hydrothermal synthesis) and combustion method are also widely used.

Some of the typical reactions that occur in oxide synthesis:



Another route is to obtain a solid product from a gas phase reaction. MgO and Cr_2O_3 do not react to form MgCr_2O_4 , but Cr_2O_3 reacts with O_2 , giving $\text{CrO}_3(\text{g})$, which can react with MgO .



- Difficult to guarantee a single-phase product.
- Different phases in the product are hard or impossible to separate.

Despite of these shortcomings the technique is widely used and quite successful for cation substitution reactions. Improvements can be obtained by smaller particles size ($<1\mu\text{m}$ instead of $10\mu\text{m}$), e.g. by spray-drying, freeze-drying, co-precipitation.

1.2.2 Precursor Method

The diffusion length problem of solid-state reactions can be avoided if the necessary cations can be included in a suitable precursor. Oxide is formed by the decomposition of the precursor:

Precursor	Product
LaCo(CN) ₆ .5H ₂ O	LaCoO ₃
LaFe(CN) ₆ .6H ₂ O	LaFeO ₃
Ba[TiO(C ₂ O ₄) ₂]	BaTiO ₃
Li[Cr(C ₂ O ₄) ₂ (H ₂ O) ₂]	LiCrO ₂
M ₃ Fe ₆ (CH ₃ -COO) ₁₇ O ₃ OH.12C ₅ H ₅ N	MFe ₂ O ₄ Spinel

Organometallic precursors, especially carboxylates and alkoxides, used for synthesis of some of the perovskite oxides have been reviewed by Chandler et al. [3]. Many metals can be combined in a precursor by using carbonates. Various carbonates have a similar calcite structure and can be readily prepared as solid solutions. During heating in nitrogen or vacuum, an oxide $\text{Mn}_{1-x}\text{M}_x\text{O}$ is formed. The oxide has a rock salt structure. Metals that have been used include Mg, Mn, Fe, Zn, Ca, Co, Cd. The simple oxides can be used as precursors for further synthesis.

1.2.3 Topochemical Reactions

Hydrogen can be intercalated into various oxides. Iodine has been intercalated into high-Tc oxides like $\text{Bi}_2\text{CaSr}_2\text{Cu}_2\text{O}_8$ without destroying superconductivity.

1.2.5 Sol-Gel Synthesis

This method avoids the problems of powder ceramic synthesis. The process involves steps as follows:

1. Prepare a sol: a colloidal suspension of inorganic precursor in a liquid (Alkoxysilane).
2. Adjust the pH of the solution to promote the formation of a gel
3. Dry the gel, forming a xerogel (or an aerogel or cryogel)
4. Sinter

Advantages of the sol-gel technique:

- ❖ Precursors are very finely mixed
- ❖ Relatively easy to adjust the stoichiometry
- ❖ Can be used for coating, thin films
- ❖ Due to the small particle sizes, processing temperatures can be relatively low.

1.2.6 High-Pressure Synthesis

High pressures are used for the synthesis of phases that would not otherwise form. The free energy is affected by the following processes.

1. Pressure delocalizes outer d electrons by increasing orbital overlap.

LiMnO_2 has been prepared by the ion exchange reaction of NaMnO_2 and LiCl or LiBr in hexagonal [5].

1.2.8 Alkali Flux and Electrochemical Method

Use of strong alkaline media in the form of either solid fluxes or molten solutions has enabled the synthesis of novel oxides. The alkali flux stabilizes higher oxidation states of the metal by providing an oxidizing atmosphere. Alkali carbonates fluxes have been used to prepare transition metal oxides such as LiNiO_3 . For example $\text{La}_4\text{Ni}_3\text{O}_{10}$ was prepared by bubbling Cl_2 gas through a NaOH solution of lanthanum and nickel nitrates.

Electrochemical methods have been employed to advantage for the synthesis of many solid materials, including oxides. Vanadate spinels of the formula MV_2O_4 as well as tungsten bronzes (A_xWO_3), have been prepared by the electrochemical route (6). Tungsten bronzes are obtained at the cathode when current is passed through two inert electrodes immersed in a molten solution of the alkali metal tungstate A_2WO_4 and WO_3 ; oxygen is liberated at the anode. Oxides containing metals in high oxidation states are prepared by electrochemical methods.

1.2.9 Crystal Growth Method

In techniques that are discussed above, result in powder samples. It is often necessary to obtain single crystals. The basic methods are:

1. Solid-Solid
2. Liquid-Solid
3. Gas- Solid (Sublimation and Sputtering)

ions) in these systems control the relative rates of these reactions. In addition, small-tunnel materials are usually more active and selective for such oxidations than large-tunnel materials. The other reactions catalyzed by manganese oxides include decomposition of several reactants. Amorphous manganese oxide materials have been found to photo-chemically and thermally decompose phosphine oxide materials that are model complexes for chemical warfare agents. Also, they have been used as catalyst for decomposition of H_2O_2 [3], for selective oxidation of cyclohexane to cyclohexanol and cyclohexanone [4], and also for the oxidative dehydrogenation of ethanol [5]. Iron oxide has been studied as selective catalyst for the production of butadiene in the partial oxidation of butane. The catalytic properties of iron and zinc cations for the water gas shift reaction: $(CO+H_2O \longrightarrow CO_2 + H_2)$ are also observed [6]. The catalytic dehydration of ethanol to ethylene was investigated using different transition metal oxides such as titanium oxide, magnesium oxide, cobalt oxide, chromium oxide [7] etc. TiO_2 is used as photo catalyst because of its high catalytic activity. Doping of TiO_2 with transition metal ions was used as a good tool to improve the photo catalytic properties and enhancement of visible light response. Do et al. and Papp et al. have published the result on the catalytic role of TiO_2/WO_3 and TiO_2/MoO_3 and found that the degradation rates of 1, 4-dichlorobenzene was enhanced significantly [8].

1.4.2 Superconductor

The superconducting oxides and metal composite oxides are provided in a variety of useful forms. A superconductor comprised of a polycrystalline metal oxide such as YBa_2CuO_{7-x} [$0 < x < 0.5$] exhibits superconducting properties [9] and capable of conducting very large current densities. Lin et al. [10] prepared Tl-Ca-Ba-Cu-o superconductor with thallium oxide. The precursor was obtained by sol-gel method from

electrodes were tested by Miura et al. [15] for detecting NO and NO₂ potentiometrically and ampero-metrically at high temperature.

1.4.5 Electrode

Several transition metal oxides are used as electrode materials. Among several transition metal oxide electrode materials for super capacitors, hydrous ruthenium oxide show a high capacity of over 700 F/g [16] and excellent cyclability in aqueous sulphuric acid. Because of its high cost, alternative metal oxide electrode materials are being developed to replace ruthenium oxide e.g., NiO_x, CoO_x, MnO₂ etc. Lithium intercalation and deintercalation in amorphous MoO₃ electrodes were investigated in situ using grazing incidence reflection mode X-ray absorption spectroscopy. Iron based oxide such as LiFeO₂ is regarded as a positive electrode material for lithium ion battery [17]. Metal electrode coated by thin oxide film (e.g. PtO_x on Pt, TiO₂ on Ti) is frequently encountered in electrochemical measurement. Li-Fe-Mn positive electrode is used in automobiles. Solid oxide fuel cell which is a ceramic device that operates at temperature range 800-1000⁰C. The design based on zirconia electrolyte with (La, Sr) MnO₃ is preferred as cathode and Ni/ZrO₂ as anode [18].

1.5 MANGANESE

Manganese is widespread in nature, but is found only in compounds, it makes up 0.091% of the Earth's crust. It is the 13th most abundant element, and the third most abundant transition element, after iron and titanium. Useful manganese deposits were formed by weathering of primary silicate sediments, and essentially contain manganese oxides.

sterility among other symptoms. Excess manganese causes irritation of the respiratory passages and impairment of movement.

1.5.4 Chemical properties

Manganese is somewhat more reactive than its neighbors in the periodic table, Cr, Tc and Fe. In compact form, it is only superficially oxidized by oxygen, but in finely divided form, it burns in air to form Mn_3O_4 . It does not form a passivating oxide layer.

1.5.5 Manganese in compounds

In its compounds, manganese is usually in oxidation state +2,+3,+4,+7(e.g. $MnCl_2$, MnO_2 , MnF_3 , Mn_2O_7). However there are also compounds in which it occurs in +5 and +6 states (e.g., MnO_4^{3-} , MnO_4^{2-}), as well as the states +1, 0,-1,-2 and -3(e.g., $Mn(CN)_6^5$, $Mn_2(CO)_{10}$, $Mn^{-1}(CO)_5^-$, Mn-II (phthalocyanin) and Mn-III(NO_3)(CO)). The +2 and +7 oxidation states are very important. The basicity of the oxides in water decreases with increasing Mn valence, while their acidity increases. Thus Mn(II) oxide is a base anhydride while Mn(VII) oxide is amphoteric. The manganese (II) ion, is the most important oxidation state of manganese, it has half filled 3d shell and is thus isoelectronic with Fe^{+3} . In acid solution it is particularly stable with respect to both oxidation and reduction. Manganese combines with oxygen in molecular ratio to form various oxides, hydroxides and oxide hydroxides of manganese.

The most important compounds of manganese are the oxides, MnO , Mn_2O_3 , MnO_4 , and MnO_2 , potassium permanganate. They are used in the production of pigments, metal soaps, magnets, dry cells, corrosion protection, as additives to feed and fertilizers, and as oxidizing agents in organic synthesis, water treatment; exhaust gas purification, oxidimetry and medicine.

MnO is produced on heating the higher oxides in flowing oxygen or upon thermal decomposition of Mn(II) carbonate or oxalate in H₂ or N₂ atmosphere [31]. Also it is produced from manganese dioxide and coke at 400-1000⁰C. Decomposition of Mn₂(CO)₈ also gives MnO with Mn₂O₃ as impurity [32]. MnO nanocrystals capped with organic ligands is prepared by decomposition of manganese acetate in a mixture of triethylamine and oleic acid [33]. MnO is also prepared by decomposition of manganese acetyl acetonate in oleylamine [34]. MnO with average diameter 6-14 nm has been prepared by decomposition of manganese cupferronate {Mn(C₆H₅N₂O₂)₂} in presence of trioctylphosphineoxide (TOPO) under solvothermal conditions [35]. Decomposition of Mn(cup)₂ at 325⁰C in toluene in presence of TOPO as capping agent gives MnO.

1.5.6.2 Diamanganese Trioxide

Manganese sesquioxide (Mn₂O₃) is obtained in its α-form, on heating Mn(IV) oxide in air to above 550⁰C, as brown powder. On further heating to over 900⁰C, it is converted into reddish brown trimanganese tetraoxide, Mn₃O₄ Oxide, which is found in nature as hausmannite. The black γ-form of Mn(III) oxide is obtained by oxidation of freshly precipitated Mn(OH)₂ in air followed by drying the resulting hydrate Mn₂O₃.xH₂O, above 500⁰C. An intermediate hydrate is manganese oxide hydroxide. The latter occurs in nature as manganite. At 300-500⁰C, MnO(OH) is converted to Mn₅O₈ which can also be obtained by heating Mn₃O₄ in air at 250-550⁰C [31].

Manganese (II) acetylacetonate [CH₃COCH=COCH₃]₂Mn and manganese (III) acetylacetonate [CH₃COCH=COCH₃]₃Mn are dissolved in acetone at room temperature. The SBA- 15 powder is then added into solution after Mn compounds have dissolved completely. The precursors are obtained by stirring until solvent evaporates. The obtained precursor is then washed with acetone. This is followed by calcinations in air at 773K for

ethanol and finally dried at 60⁰C in air. Hydrothermal reaction between Mn₂O₃ and NaOH for a long duration also gives MnO₂ [42].

1.5.7 Applications of Manganese Oxide

MnO₂ is used as depolarizer in dry cells (especially zinc-carbon and leclanche's cells), as a pigment for bricks (red to brown to grey), as an oxidizing agent (e.g. for producing hydroquinone from aniline, or in the production of polysulphide rubbers), as a catalyst for oxygen transfer, in the production of manganese (II) salts such as MnSO₄ and as glassmaker's soap. These oxides are used as electrochromic materials. They have a wide range of applications in catalysis and battery technologies [43]. Among the series of manganese oxides Mn₃O₄ is known to be an active catalyst in various oxidation and reduction reactions e.g., it can be used as a catalyst for the oxidation of methane and carbon monoxide or the selective reduction of nitrobenzene [44]. Moreover the catalytic application of Mn₃O₄ has been extended to the combustion of organic compounds at temperatures of the range 373-773K [45]. Polymorphs of Mn₂O₃ have been used as catalysts for removing carbon monoxide and nitrogen oxide from waste gas [46]. Mn₂O₃ is used as an electrode material for rechargeable lithium batteries [47].

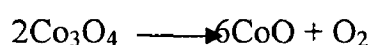
1.6 COBALT

Cobalt is a ferromagnetic metal. Pure cobalt is not found in nature, but compounds of cobalt are common. Small amounts of it are found in most rocks, soil, plants, and animals. It is the element of atomic number 27. The Curie temperature is 1388 K, and the magnetic moment is 1.6-1.7 Bohr magnetons per atom. In nature, it is frequently associated with nickel, and both are characteristic minor components of meteoric iron. Metallic cobalt occurs as two crystallographic structures: hcp and fcc. The ideal transition temperature between hcp and fcc structures is 722K, but in practice, the energy difference

1.6.4 Cobalt oxides

Cobalt (II) Oxide

It appears as olive-green to red crystal, or grayish or black powder. It is used extensively in the ceramics industry as an additive to create blue colored glazes and enamels as well as in the chemical industry for producing cobalt(II) salts. CoO crystals adopt the rock salt structure with a lattice constant of 4.2615Å. Cobalt (II) oxide is anti-ferromagnetic below 16⁰C. Cobalt (II,III) oxide decomposes to cobalt (II) oxide at 950⁰C.



Cobalt (II) Oxide

Cobalt (III) Oxide, Co₃O₄, is a black substance that could be obtained by adding cobalt (II) nitrate to an aqueous solution of sodium hypochlorite (also known as bleach). In that case, it is used as a catalyst to speed up chemical reaction.

Cobalt (II, III) Oxide

This oxide has a chemical formula as Co₃O₄. It is a black solid, and mixed valence compound, containing both Co(II) and Co(III) oxidation states. It can be formulated as Co^{II}Co^{III}₂O₄ or CoO.Co₂O₃. Co₃O₄ adopts the normal spinel structure, with Co²⁺ ions in tetrahedral interstices and Co³⁺ ions in the octahedral interstices of the cubic close-packed lattice of oxide anions.

1.6.5 Chalcogen compounds

Several oxides of cobalt are known. Green cobalt (II) oxide (CoO) has NaCl structure and is readily oxidized with water and oxygen to brown cobalt (III) hydroxide [Co(OH)₃]. At temperatures of 400-500⁰C the CoO is oxidized to the blue cobalt (II,III)

Cobalt and its compounds, especially cobalt carboxylates, are good oxidation catalysts. They are used in paints, varnishes, and inks as drying agents through the oxidation of certain compounds. The same carboxylates are used to improve the adhesion of the steel to rubber in steel-belted radial tires.[52].

1.7 ZINC

Zinc is the 23rd most abundant element in the earth's crust. The most heavily mined ores tend to contain roughly 10% iron as well as 40-50% zinc. It occurs in two oxidation states +1 (rare) and +2 with hexagonal crystal structure.

1.7.1 Isotopes

Naturally occurring zinc is composed of the 5 stable isotopes ^{64}Zn , ^{66}Zn , ^{67}Zn , ^{68}Zn , and ^{70}Zn with ^{64}Zn being the most abundant. This element also has four Meta states.

1.7.2 Compounds

Zinc oxide is the best known and most widely used zinc compound, as it makes a good base for white pigments in paint. It also finds industrial use in the rubber industry, and is sold as opaque sunscreen. A variety of other zinc compounds find use industrially, such as zinc chloride (in deodorants), zinc pyrithione (anti-dandruff shampoos), zinc sulfide (in luminescent paints), and zinc methyl or zinc diethyl in the organic laboratory [53].

1.7.3 Electrochemistry

Electrochemical properties of zinc make it a good material for anode materials. Zinc is used as part of batteries. The most widespread such use is as the anode in alkaline batteries [54]. Zinc is used as the anode or fuel of the zinc-air battery/fuel cell providing the basis of the theorized zinc economy [55].

on substrates with cubic lattice structure. In both cases, the zinc and oxide are tetrahedral. The rocksalt NaCl-type structure is only observed at relatively high pressures 10GPa.[57]

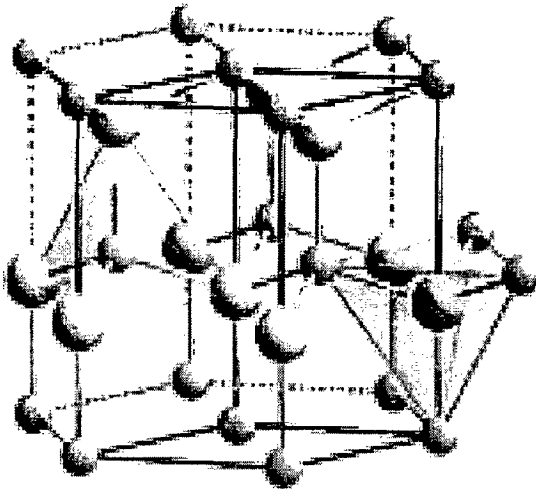


Fig: 1.7.1 Wurtzite Structure

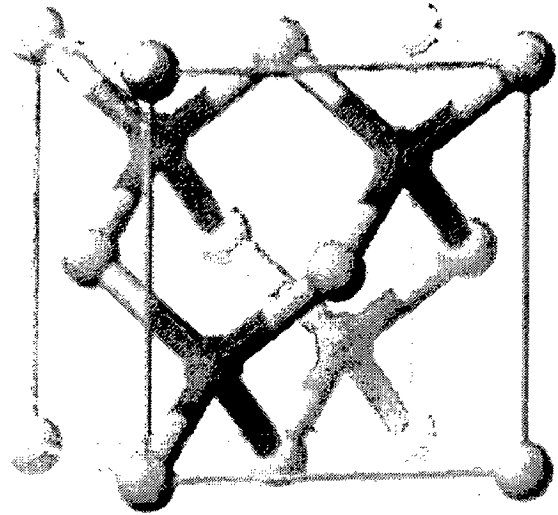


Fig:1.7.2 A Zincblende unit cell

None of these three ZnO structures possesses inversion symmetry (reflection of a crystal relatively any given point does not transform it into itself). This important property results in piezoelectricity, pyroelectricity and spontaneous polarization of zinc oxide.

1.7.7 Mechanical Properties

Among the tetrahedrally bonded semiconductors, it has been stated that ZnO has the highest piezoelectric tensor or at least one comparable to that of GaN and AlN. This property makes it a technologically important material for many piezoelectrical applications, which require a large electromechanical coupling.

1.7.8 Electronic properties

ZnO has a relatively large direct band gap of $\sim 3.3\text{eV}$ at room temperature; therefore, pure ZnO is colorless and transparent. Advantages associated with a large band

oxide removes significant amounts of HCN and H₂S from tobacco smoke without affecting its flavor.

1.7.9.4 Zinc oxide nanorod sensor

Zinc oxide nanorod sensors are devices detecting changes in electrical current passing through zinc oxide nanowires due to adsorption of gas molecules. Selectivity to hydrogen gas was achieved by sputtering Pd clusters on the nanorod surface. The addition of Pd appears to be effective in the catalytic dissociation of hydrogen molecules into atomic hydrogen, increasing the sensitivity of the sensor device. The sensor detects hydrogen concentrations down to 10 parts per million at room temperature, whereas there is no response to oxygen.

1.8 AIM OF THE PROJECT

According to literature survey, many transition metal oxides constitute an important class of compounds as they possess properties suitable for catalyst, superconductor, adsorbent, sensor and electrodes. There are various uses of transition metal oxides as electrode material, catalyst, electrochromic material, depolarizer in dry cells, pigment for bricks, oxidizing agents, additives to feed and fertilizers and also in production of magnets etc. Several applications of manganese oxides, cobalt oxides and zinc oxides have been stated in 1.5, 1.6 and 1.7 sections respectively. In view of the above, it is proposed to study more about these oxides.

Due to their low cost, low toxicity and environmentally friendly character, these transition metal oxides are very promising material as electrode materials in super – capacitors and catalyst. Several studies have been carried out on amorphous or nano-crystallized MnO₂, ZnO, and Co₃O₄ compounds obtained by precipitation method. These

CHAPTER-2

EXPERIMENTAL

2.1 MATERIALS USED

The materials used for carrying out experiments:

S.No.	Compounds	Marketed by	Grade
1.	Manganese Nitrate	E-Merck	LR
2.	Cobalt Nitrate	E-Merck	LR
3.	Zinc Nitrate	E-Merck	LR
4.	Ammonia Liquid	Rankem	LR

All the chemicals used in this synthesis were used as received without further purification.

2.2 EQUIPMENTS USED

Characterization and structural elucidation of the synthesized oxides were performed using techniques like powder X-ray diffraction, Thermo gravimetric analysis (TGA), and Magnetic Susceptibility Measurement Using SQUID and Scanning electron microscopy (SEM).

2.2.1 Thermo Gravimetric Analysis - Differential Thermal Analysis

The TGA/DTA curves were recorded on a Perkin Elmer (Pyris Diamond) TGA-DTA High Temperature 115 instrument at Institute Instrumentation Centre (IIC), IIT Roorkee under the following conditions:

The mean crystallite size was calculated from the XRD pattern using Deby-Scherrer equation [48]. Deby-Scherrer Formula is-

$$D = 0.9 \lambda / \beta \cos \theta$$

Where, λ = X-Ray wavelength

β = Full Width at half maxima (FWHM in radians)

θ = Bragg's angle

D = Mean crystallite size (\AA)

2.2.3 Field Emission-Scanning Electron Microscopy (FE-SEM)

To observe the morphology and particle size FE-SEM analysis were made. The instrument used for conducting FE-SEM was QUANTA 200 FEG made by NEI Netherlands. High voltage (20kV) electron beam was produced by using Field Emission Gun (FEG). The detector used for identifying back scattered electron beam was Secondary Electron Detector (SED). EDAX was used for semi quantitative analysis. The detector used for EDAX was Si-Li detector (X-ray detector). This equipment was available at Institute Instrumentation Centre, IIT Roorkee.

2.2.4. SQUID

The magnetic studies were carried out using SQUID (Superconducting Quantum Interference Device). It was Quantum Design MPMS XL model available at Institute Instrumentation Centre, IIT Roorkee. The conditions used were as follows:

Field ----- 10000 Gauss

Temperature ----- 10 K – 200 K

2.3 SYNTHESIS OF MANGANESE OXIDE

The synthesis of manganese oxide was carried out using precipitation method [48]. The manganese oxide was synthesized by mixing 500 mL of aqueous solution of 0.1M

A flow chart detailing the synthesis of manganese oxides is shown below:

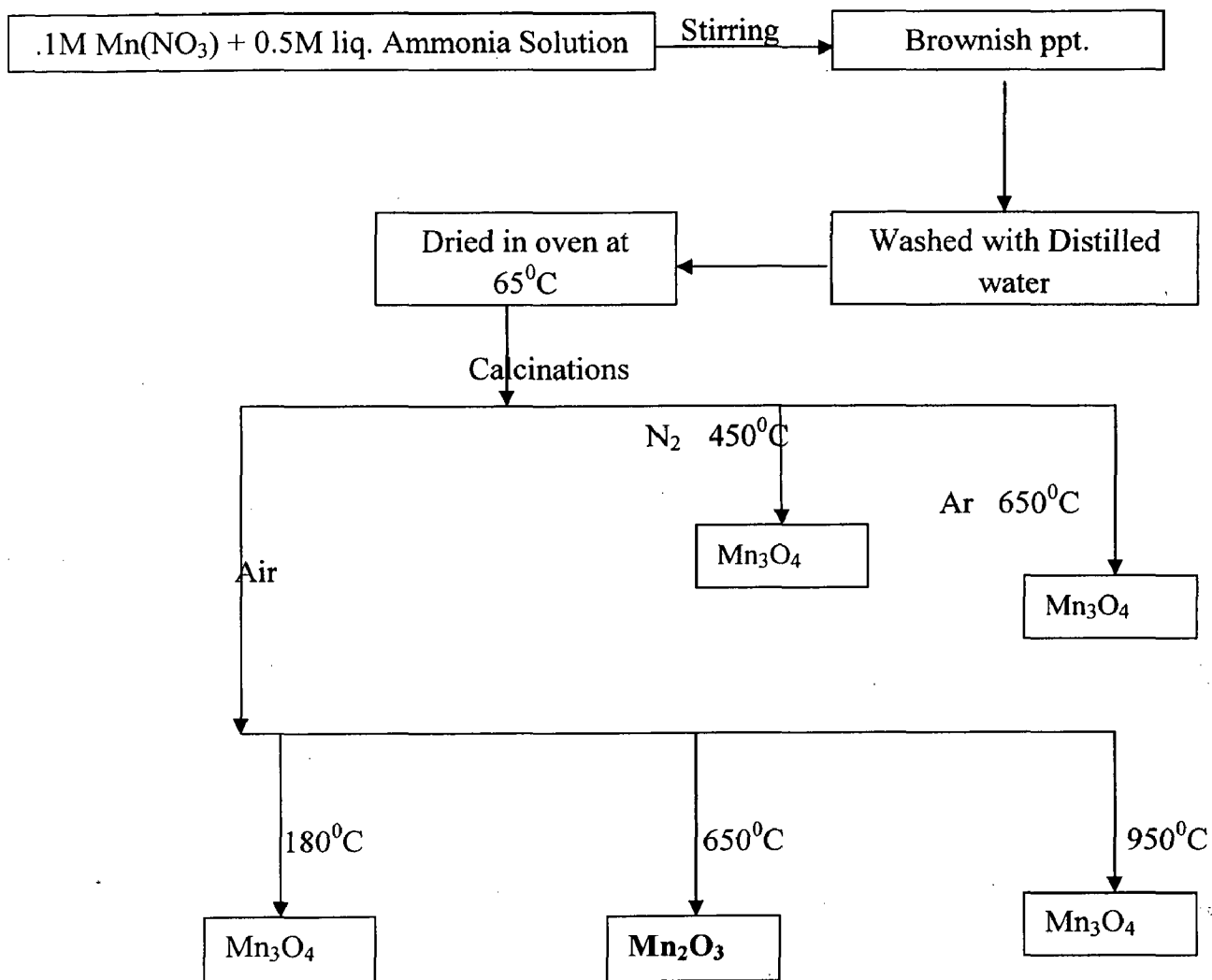


Fig: 2.1 Synthesis of various oxides of Manganese

A flow chart detailing the synthesis of Cobalt oxides is shown below:

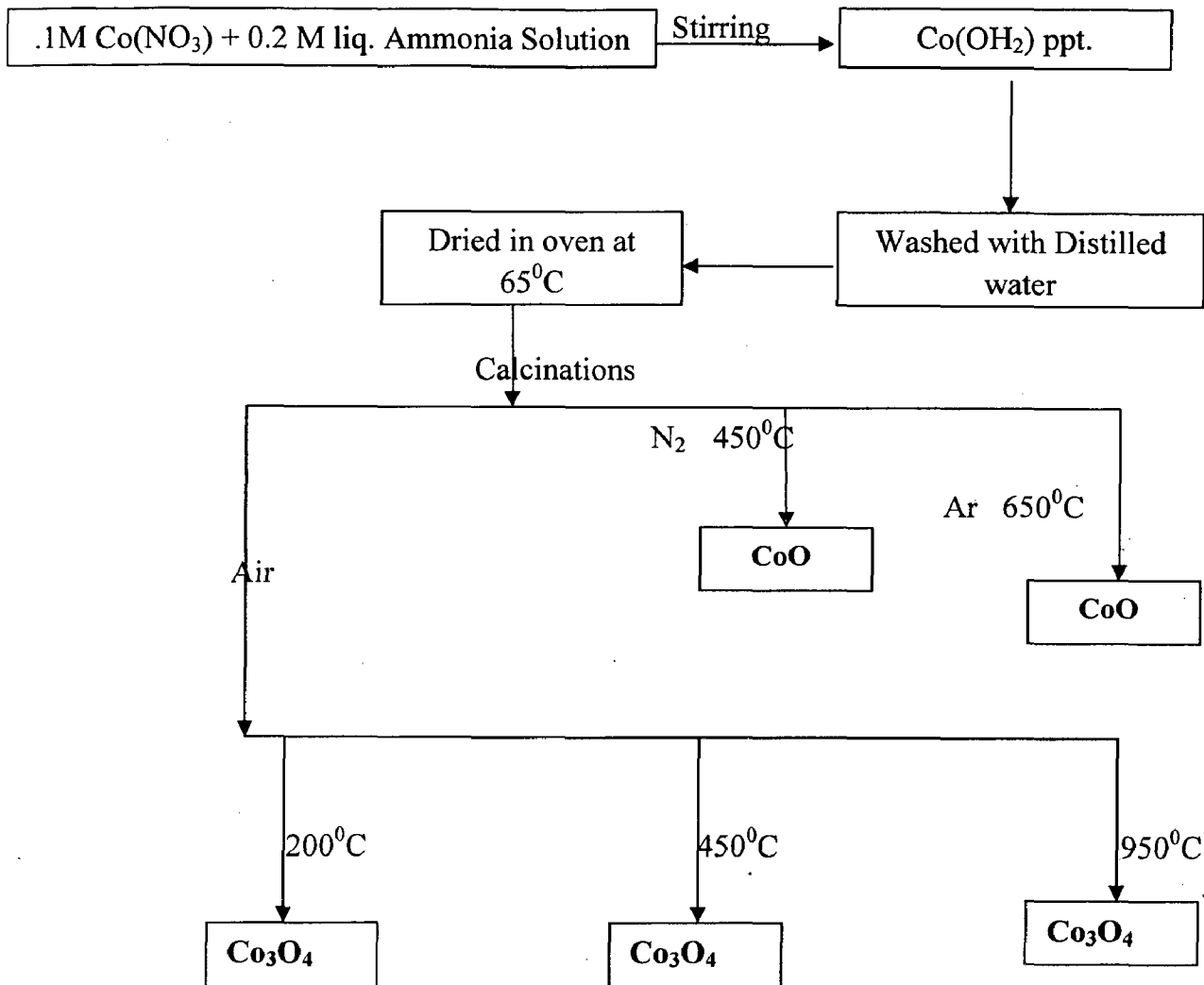


Fig: 2.2 Synthesis of various cobalt oxides

A flow chart detailing the synthesis of Zinc oxides is shown below:

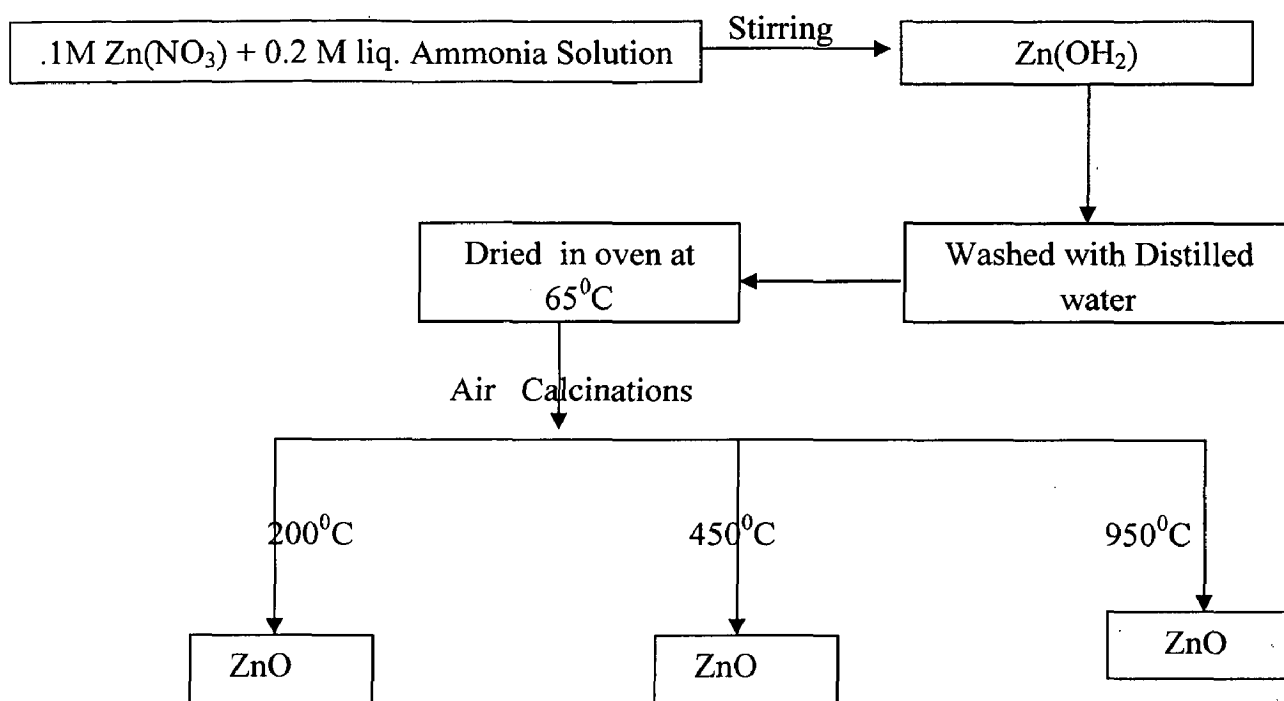


Fig: 2.3 Synthesis of various zinc oxides

RESULT AND DISCUSSION

All synthesized transition metal oxides namely; manganese, cobalt and zinc oxides were characterized using different techniques as given below:

3.1 Thermo Gravimetric Analysis–Differential Thermal Analysis

Thermo gravimetric analysis is the technique in which the mass of the sample in a controlled atmosphere is recorded continuously as a function of temperature or time as the temperature of the sample is increased. Air or inert atmosphere such as helium or argon is used for the measurement. TG curves are applied for transitions that involve decomposition, dehydration, oxidation reaction and physical processes like vaporization, sublimation, desorption etc. This technique is used for to know about thermal stability, composition of initial sample and intermediate compound that may be formed. TGA curves are characteristic of physical transitions and chemical reactions that occur over definite temperature range [59].

In Differential thermal analysis (DTA) the difference in temperature between a substance and a reference material is measured as a function of temperature while the substance and the reference material are subjected to a controlled temperature program. The temperature of the sample T_s increases linearly with time. The difference in temperature ($\Delta T = T_r - T_s$) is monitored and plotted against temperature to give a differential thermogram. DTA peaks result from both physical changes and chemical reactions induced by temperature changes in the sample. Exothermic process shown by a maximum whereas a minima is corresponds to an endothermic process [59].

Each crystalline substance has a unique X-ray diffraction pattern with specified d-values and the relative peak intensities. The diffracting phase in a sample can be identified.

The different X-ray diffractograms of precursors and different forms of oxides of manganese, cobalt and zinc are shown in the Figure [4-9], [12-17] and [18-21] respectively.

The X-ray diffraction data for each of above mentioned compounds are given in tables [7-21].

3.2.1 X-RAY DIFFRACTION ANALYSIS OF MANGANESE OXIDES

The precursor of different manganese oxides is obtained by hydrolysis of manganese nitrate salt by liquid ammonia. This precursor was heated under different temperatures and atmospheres. Results obtained are discussed below:

The X-ray diffraction pattern shown in Fig.4 of different manganese oxide shows that the manganese oxide Mn_3O_4 formed is tetragonal in shape at room temperature in air.

The oxide formed due to the calcinations at $180^{\circ}C$ in air atmosphere is a Mn_3O_4 tetragonal system. The Cell parameters for the Mn_3O_4 are,

$a= 5.7621$, $b=1.6434$ and $c=9.4696$ (Fig. 5)

Similar results were obtained with Mn_3O_4 when calcinated at $1000^{\circ}C$ (Fig. 7). Calcination of Mn_3O_4 $650^{\circ}C$ gave all different result in the form of Mn_2O_3 which exist in orthorhombic crystal system. The observed cell parameters are,

$a= 9.4118$, $b=9.4177$ and $c=9.4233$ (Fig. 6).

When the precursor of Mn_3O_4 is treated in the N_2 and Ar environment the results are same as obtained when calcinated at $180^{\circ}C$ & $1000^{\circ}C$ (Fig. 8 & 9).

Fig. 18 indicates that the precursor of zinc oxide formed is ϵ -Zn(OH)₂ which shows its presence in orthorhombic system. The cell parameters are-

$$a=8.490, b=5.162 \text{ \& } c=0.9525$$

When this precursor is heated in presence of air at different temperatures 200⁰C, 450⁰C & 950⁰C respectively the result obtained shows that ZnO which is in Hexagonal crystal system (Fig. 19-21).

The XRD data from the line broadening experiments helped to calculate the particle size. Particle size is determined using the Scherrer formula.

$$D = 0.89\lambda / \beta \cos \theta$$

Where, λ = X-Rays wavelength (1.5418 Å)

β = Full Width at half maxima (Radians)

θ = Bragg's angle

D = Crystallite size (Å)

We got the particle size of the synthesized oxides in the nano range. The sizes of the particles are given in Table [21].

3.3 SQUID

The magnetic susceptibility of the samples of manganese precursor as a function of temperature was recorded using superconducting quantum interference device (SQUID). The plots for magnetization vs. temperature were plotted for each and are shown in Figures (10-11). The magnetization plot for manganese oxides formed in nitrogen and argon environment is shown in Figure 10 and Figure 11 respectively. In our

CONCLUSION

Manganese, cobalt and zinc oxides were prepared in nanocrystalline size using precipitation method. All precursors of oxides were calcined at different temperatures to get nanocrystalline oxides. These precursors and oxides were characterized by powder XRD, TGA-DTA, SQUID and SEM.

The XRD studies show that different oxides can be prepared using a single precursor. Mn_3O_4 formed at room temperature changes to Mn_2O_3 when heated to $650^{\circ}C$ in air atmosphere. Co_3O_4 is formed at $200^{\circ}C$ and $950^{\circ}C$ in presence of air from the cobalt hydroxide whereas CoO is formed at $650^{\circ}C$ but in argon atmosphere from the same precursor. Zinc oxide showed a variation in size with the temperature. The size of zinc oxides in the temperature range of $200^{\circ}C$ to $950^{\circ}C$ was 23.80 – 43.97nm. The other oxides of manganese and cobalt also showed similar results with temperature. These all synthesized oxides have the particle size, as calculated from Debye-Scherrer equation, was in nano meter. Size of particle also changes with the changing atmosphere of calcinations like nitrogen and argon. The particle size is smaller in nitrogen atmosphere as compare to argon atmosphere. In FE-SEM images the particles look agglomerated with irregular morphology.

References

1. V.E.Henrich and P.A.Cox, *The surface Science of Metal Oxides*, Cambridge University Press, 2000, P.15.
2. C.D.Chandler, C.Roger, and M.I.H. Smith, *Chem Rev.*, **93**, 1205 (1993).
3. C.N.R.Rao, B.Raveau, "Transition Metal Oxides", Wiley, New York, 1998.
4. A.R.Armstrong and P.G. Bruce, *Nature*381, 497(1996).
5. http://en.wikipedia.org/wiki/chemical_synthesis.
6. M.S. Whittingham and R.A.Huggins, in *Solid State Chemistry*, U.S. National Bureau of standards, Washington, DC,1972.
7. P.Madhudsudhan Rao, B.Viswanathan, R.P. Viswanath, *J.Mater.Sci.***30**, 4980 (1995).
8. H.Zhou, Y.F.Shen, J.Y. Wang and X.Chan, *J Catal.* **176**, 321-328 (1998).
9. J.Y.Wang, G.G. Xia and Y.G. Yin, *J. Catal.*, **176**, 275-284 (1998).
10. H.Zhou, J.Y. Wang and X. Chem, *Microporous Mesoporous Mater.*, **21**, 315-324 (1998).
11. D.G. Rethwisch and J.A. Dumesic, *J. Catal.*, **101**, 35-42 (1986).
12. T.Zaki, *J.Colloid Interface Sci.*, 284, 606-613 (2005).
13. A.Travert, O.V. Monoilova and A.A. Tsyganen Ko, *J. Phys. Chem. B.*, **106**, 1350-1362 (2002).
14. Fundamental principles of metal oxide based chemical sensors Nicolae Barsan (*Inst. of Phys. Theor. Chemistry, University of Tuebingen*)
15. N.Miura, G.Lu and N. Yamazone, *Sens. Actuators B.*, **52**, 169-178 (15 Sept. 1998).
16. K.H. Kim and K.B. Kim, *Electrochem. Org.*, ECS 210 th meeting, Abstract 0130.pdf.

31. Holleman-Wiberg, *Inorganic Chemistry*, 34th Ed., Walter de Gruyter GmbH Co. KG, D-10785 Berlin, 1995, P.1409-1413.
32. G.H. Lee, S.H. Huch, J.W. Jeong, B.J. Choi, S.H. Kim and H.C. Ri, *J. Am. Chem. Soc.*, **124**, 12094 (2002).
33. M. Yin and S. O'Brein, *J. Am. Chem. Soc.*, **125**, 10180 (2003).
34. W.S. Seo, H.H. Jo, K. Lee, B. Kim, S.J. Oh and J.T. Park, *Angew Chem Int Ed.*, **43**, 1115 (2003).
35. Moumita Ghosh, Kanishka Biswas, A. Sundaresen and C.N.R. Rao, **10**, 1039 (2006).
36. Yi Fan Han, Geng Xi chen, Zi-Yi Zhong, Kanaparthi Ramesh, Effendi Widjija and Lu-Wei Chen, *Catalysis Communication*, **7**, 739-744 (2006).
37. Shao Changlu, Guan Hongyu, Liu Yinchun, Li Xiliang and Yang Xinghua, *J. Solid State Chem.*, **177**, 2628-2631 (2004).
38. S. Mann, N.H.C. Sparks, G.H.C. Scott, *Applied and Environmental Microbiology*, **54**, 2140-2143 (Aug.1998).
39. S.Zhu and H. Zhou, *Adv. Functional Materials*, **15**, 381-386 (2004).
40. Yonglan Luo, *Material letters*, **61**, 1893-1895 (2007).
41. Xu Chun Song, Yang Zhao and Yi Fan Zheng, *J. Am. Chem. Soc.*, **7**, 159-162 (2007).
42. R.H. Ma, Y. Bando, L.Q. Zhang and T. Sasaki, *Adv. Mater.*, **16**, 918-922 (2004).
43. O. Giraldo, S.L. Brock, W. S. Willis, M. Marquez and S.L. Suib, *J. Am. Chem. Soc.* **122**, 9330 (2000).
44. J. M. Taraseon and M Armard, *Nature*, **414**, 359, 359 (2001).
45. M.Baldi, E. Finnochio, F. Milella and G. Busca, *Appl. Catal. B*, **16**, 43 (1998).
46. M.Baldi, *Appl. Catal. B.*, **17**, L175 (1998).

57. S.Mahmud et al. "nanostructure of ZnO fabricated via French process and its correlation to electrical properties of semiconducting varistors" J.Syn. React. Inorg. Met-Org and Nano Metal Chem.36 (2006)155.
58. Greenwood,Norman N; earnshaw,A.(1997),Chemistry of the Elements (2nd ed.), oxford:Butterworth-Heinemann, ISBN 0-7506-3365-4.
59. Skoog, Holler, Niemen, Principles of Instrumental Analysis, 5th Ed., Thomson, Brooks/Cole, 2004, p.798-803.

Table 4: Weight loss for Manganese Oxides Precursor (From TGA data)

S.No	Temperature (°C)	% Weight Loss (Calculated)	% Weight Loss (Theoretical)
1.	950	Low impurities	3.5

Table 5: Weight loss for Cobalt Oxides Precursor (From TGA data)

S.No	Temperature (°C)	% Weight Loss (Calculated)	% Weight Loss (Theoretical)
1.	650	11.12	11.21
2.	950	Low impurities	5.37

Table 6: Weight loss for Zinc Oxides Precursor (From TGA data)

S.No	Temperature (°C)	% Weight Loss (Calculated)	% Weight Loss (Theoretical)
1.	200	18.03	16.2

Table 8: X-Ray Diffraction data for Manganese oxide (Air/180°C)

S.No.	d - value (Å)		I/I ₀ x 100	
	Experimental	Literature	Literature	Literature
1.	2.49162	2.4871	100	100
2.	1.54487	1.5427	65	50
3.	2.76819	2.7624	70	76
4.	3.09654	3.0854	40	40
5.	1.58339	1.5764	25	27
6.	2.86973	2.854	40	60

Oxide Form: Mn₃O₄

System: Tetragonal

Table 10: X-Ray Diffraction data for Manganese oxide (Air/1000⁰C)

S.No.	d - value (Å)		I/I ₀ x 100	
	Experimental	Literature	Literature	Literature
1.	2.48821	2.4871	100	100
2.	2.77027	2.7624	80	90
3.	1.54445	1.5427	65	75
4.	3.09120	3.0854	70	80
5.	1.79957	1.7945	55	60
6.	1.57668	1.5764	60	60
7.	2.03833	2.0382	45	45
8.	2.36817	2.3605	20	20
9.	2.71957	2.7624	20	20
10.	4.93817	4.9203	12	15

Oxide Form: Mn₃O₄

System: Tetragonal

Table 12: X-Ray Diffraction data for Manganese oxide (Ar/650⁰C)

S.No.	d - value (Å)		I/I ₀ x 100	
	Experimental	Literature	Literature	Literature
1.	2.49143	2.4871	100	100
2.	2.77459	2.7624	70	80
3.	1.54598	1.5427	40	60
4.	3.09502	3.0854	50	60
5.	1.57808	1.5764	30	20
6.	2.04044	2.0382	40	20
7.	1.80195	1.8262	35	30

Oxide Form: Mn₃O₄

System: Tetragonal

Table 14: X-Ray Diffraction data for cobalt hydroxide (Air/450⁰C)

Due to low crystalline at 200⁰C there is no sharp peaks obtained. Hence no table is available for the Cobalt oxide at 200⁰C.

S.No.	d - value (Å)		I/I ₀ x 100	
	Experimental	Literature	Literature	Literature
1.	2.43710	2.43	100	100
2.	2.85847	2.85	55	60
3.	1.42762	1.42	30	45
4.	2.02134	2.02	10	20

Oxide Form: Co₃O₄

System: Cubic

Table 16: X-Ray Diffraction data for cobalt hydroxide (Ar/650°C)

S.No.	d - value (Å)		I/I ₀ x 100	
	Experimental	Literature	Literature	Literature
1.	2.13266	2.13	100	100
2.	2.46463	2.46	40	46
3.	1.50575	1.50	30	50
4.	1.38935	1.30	25	28
5.	1.80271	1.81	10	15
6.	1.89483	1.89	10	12

Oxide Form: CoO

System: Cubic

Table 18: X-Ray Diffraction data for Zinc Precursor (Air/200⁰C)

S.No.	d - value (Å)		I/I ₀ x 100	
	Experimental	Literature	Literature	Literature
1.	2.48210	2.48	100	100
2.	2.82264	2.82	50	56
3.	2.61065	2.61	30	50
4.	1.62741	1.62	25	40
5.	1.47929	1.47	30	30
6.	1.38005	1.38	20	25
7.	1.91420	1.91	10	12
8.	1.36027	1.36	15	14

Oxide Form: ZnO

System: Hexagonal

Table 20: X-Ray Diffraction data for Zinc Precursor (Air/950⁰C)

S.No.	d - value (Å)		I/I ₀ x 100	
	Experimental	Literature	Literature	Literature
1.	2.49040	2.48	100	100
2.	2.83452	2.82	70	80
3.	2.61877	2.61	55	75
4.	1.63031	1.63	70	60
5.	1.48162	1.48	40	45
6.	1.38177	1.38	30	50
7.	1.91991	1.91	15	30

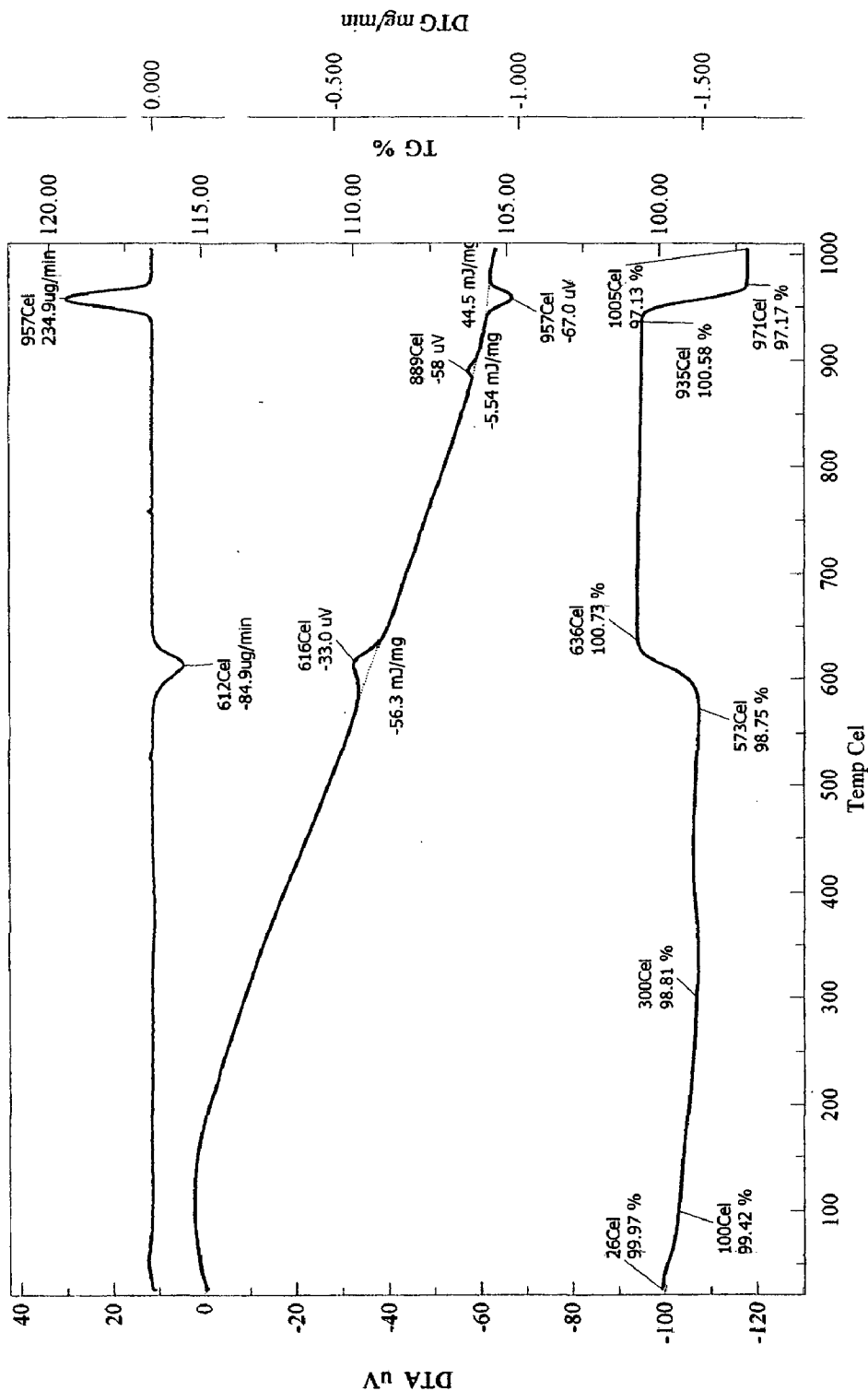
Oxide Form: ZnO

System: Hexagonal

Institute Instrumentation Centre, IITR, Roorkee.

Sample Name: JY-2
Data Name: JS-6
Measurement Date: 9/20/2008
Sample Weight: 11.16 mg
Reference Weight: 10.5 mg
Reference Name: Alumina Powder
Instrument: Perkin Elmer (Pyris Diamond)
Operator: A.K.Saini,
Pan: Alumina
Atmosphere: Air (200 ml/min)
Temperature Program:
 1* Cel 26 1000 10 0 0.5
 Cel Cel/min min s

**Fig.1 TGA-DTA graph
for Manganese oxide
precursor**

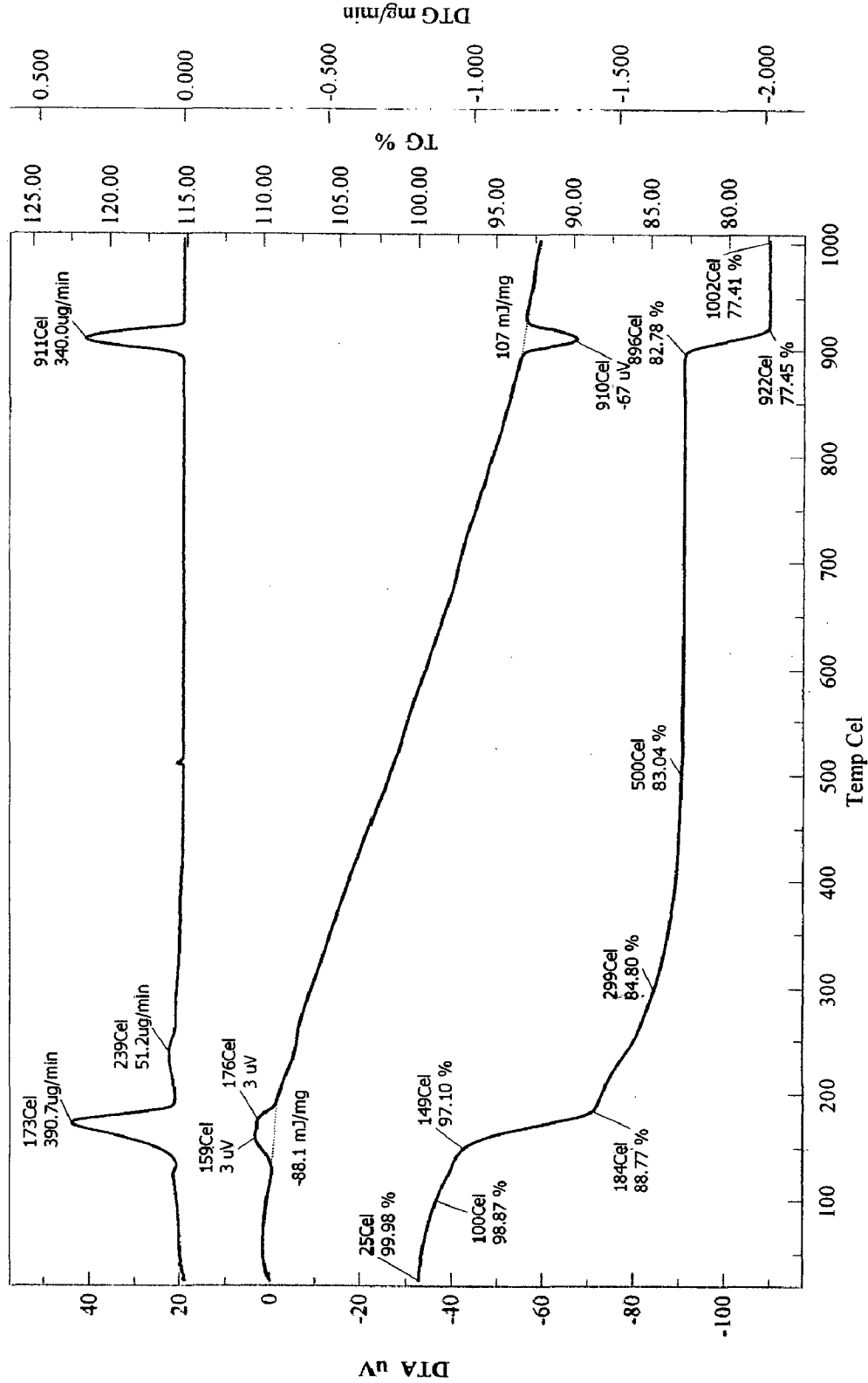


-DTA -DTG -TG

Institute Instrumentation Centre, IITR, Roorkee.

Sample Name: JY-4
 Data Name: JS-8
 Measurement Date: 9/20/2008
 Sample Weight: 10.64 mg
 Reference Weight: 10.5 mg
 Reference Name: Alumina Powder
 Instrument: Perkin Elmer (Pyris Diamond)
 Operator: A.K.Saini,
 Pan: Alumina
 Atmosphere: Air (200 ml/min)

Fig.2 TGA-DTA graph of cobalt oxide precursor



-DTA -DTG -TG

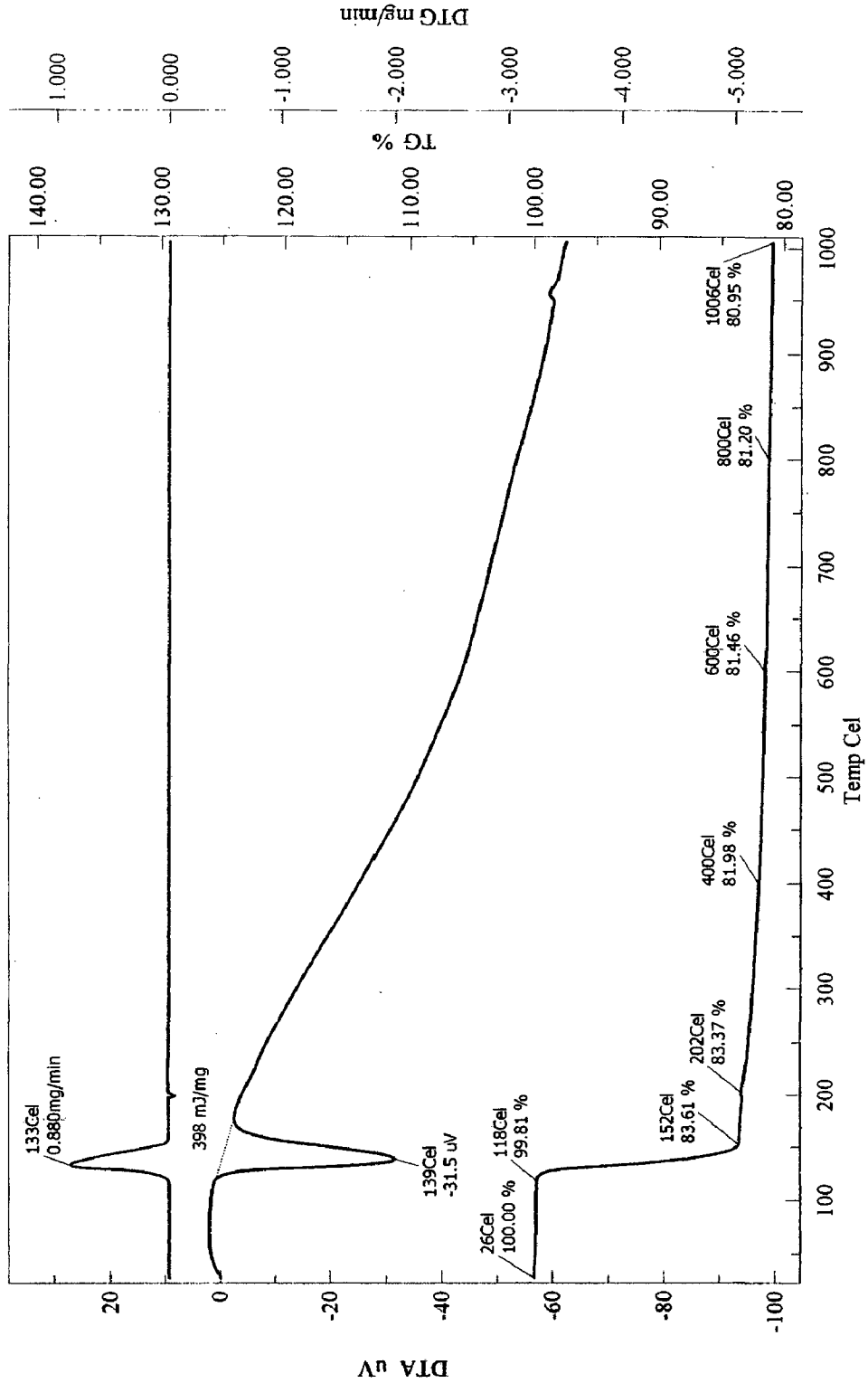
Institute Instrumentation Centre, IITR, Roorkee.

**Fig. 3 TGA-DTA graph
for zinc oxide precursor**

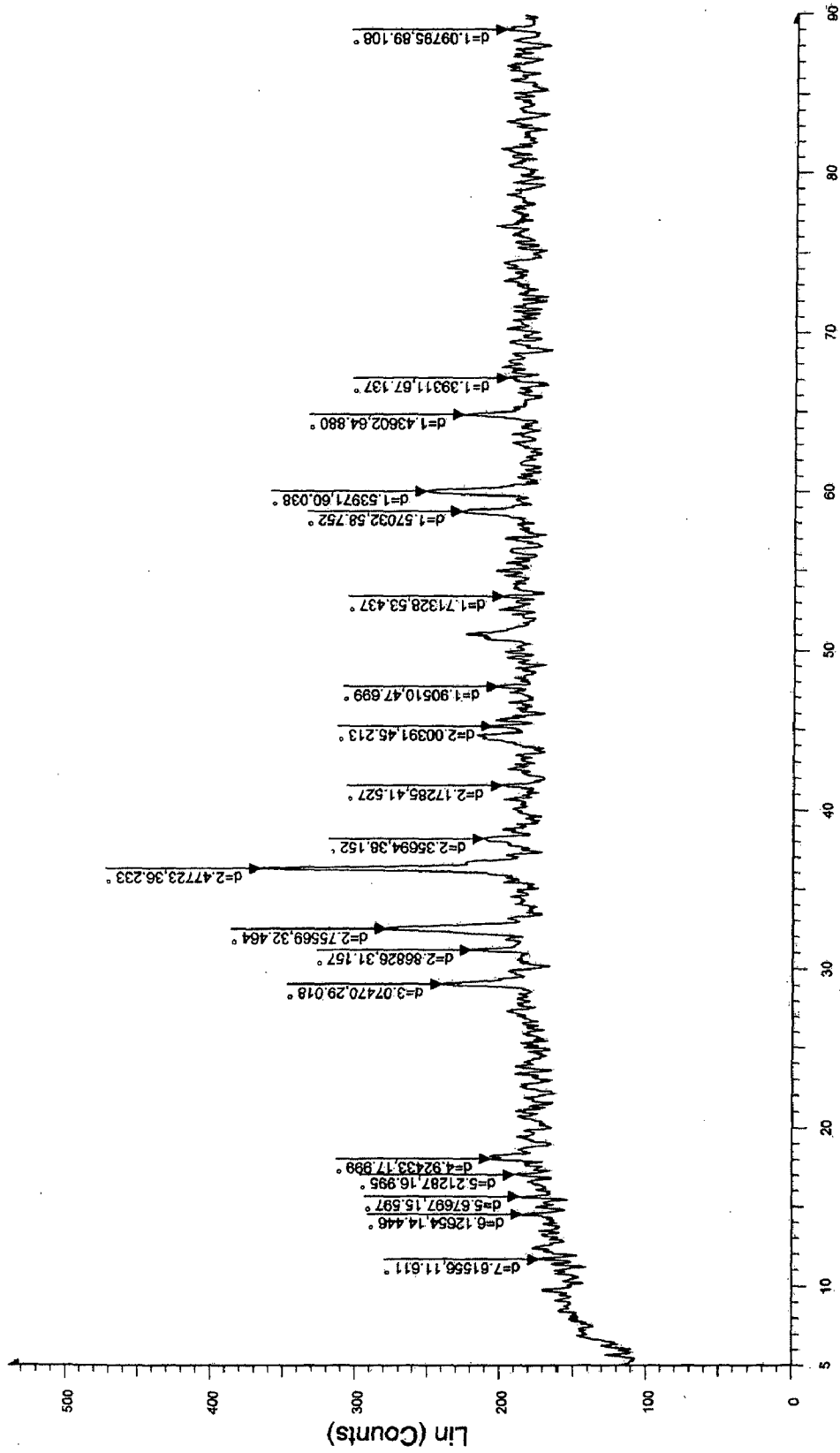
Sample Name: JY-1
 Data Name: J5-5
 Measurement Date: 9/20/2008
 Sample Weight: 10.83 mg
 Reference Weight: 10.5 mg
 Reference Name: Alumina Powder

Instrument: Perkin Elmer (Pyris Diamond)
 Operator: A.K.Saini,
 Pan: Alumina
 Atmosphere: Air (200 ml/min)

Temperature Program:
 1* 26 1000 10 0 0.5



-DTA -DTG -TG



JY-2 - File: JY-2.raw - Type: 2Th/Th locked - Start: 5.000 ° - End: 89.000 ° - Step: 0.050 ° - Step time: 0.6 s - Temp.: 25 °C (Room) - Time Started: 1222766720 s - 2-Theta: 5.000 ° - Theta: 2.50
 Operations: Smooth 0.150 | Y Scale Mult 0.750 | Import

4 XRD graph for Manganese oxide precursor at room temperature.

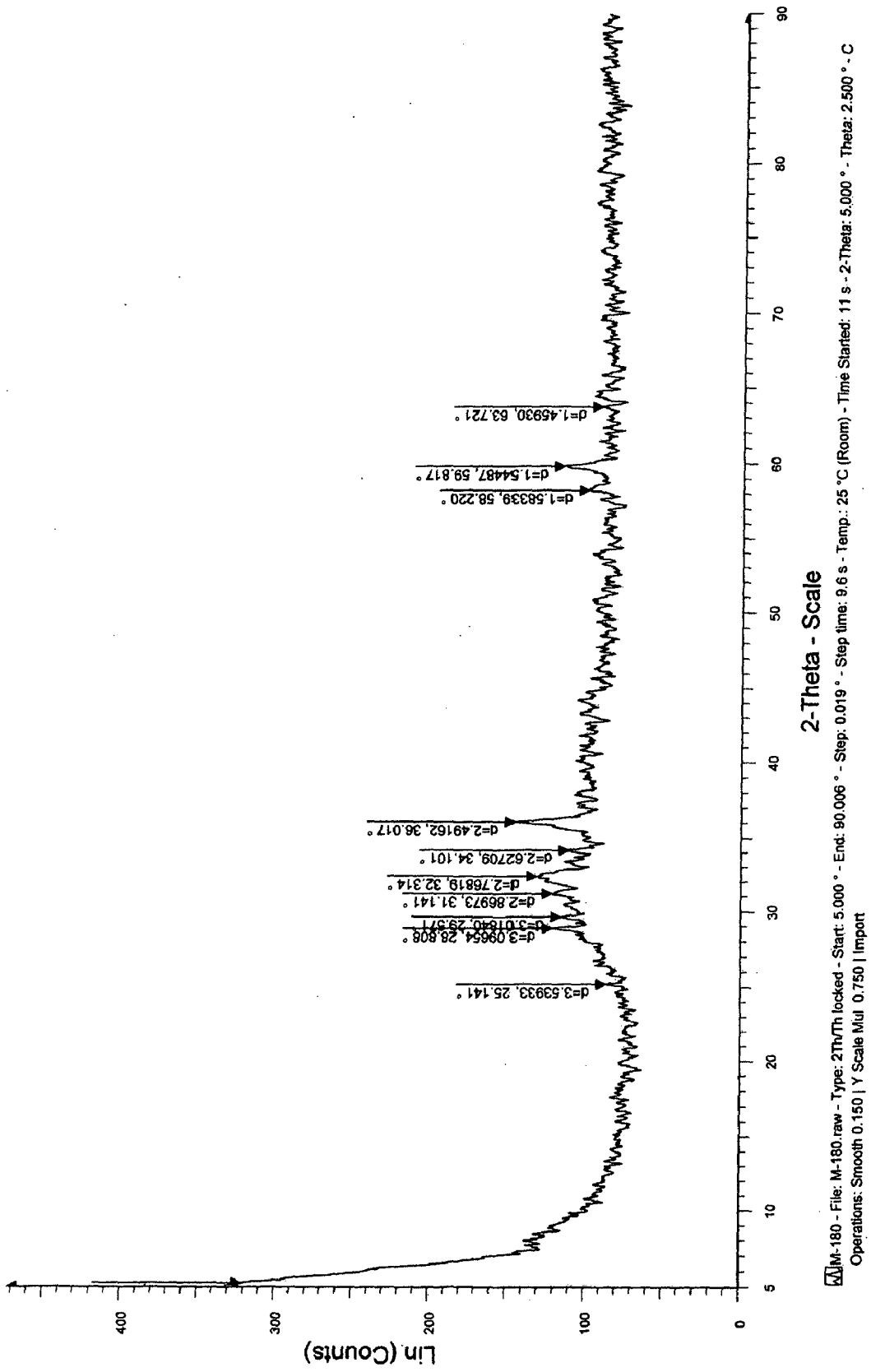


Fig. 5 XRD graph for Manganese oxide at 180°C temperature in presence of air.

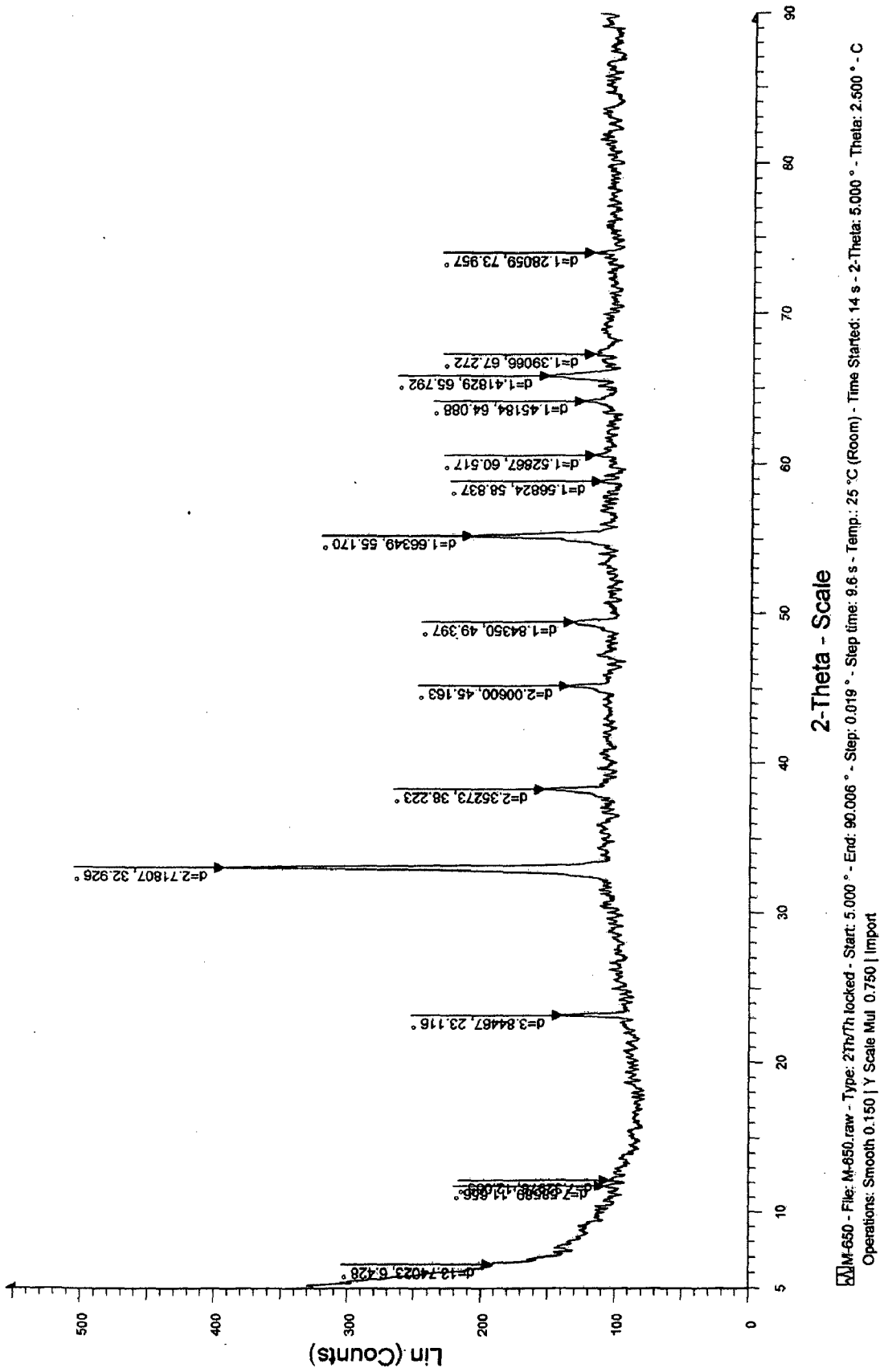
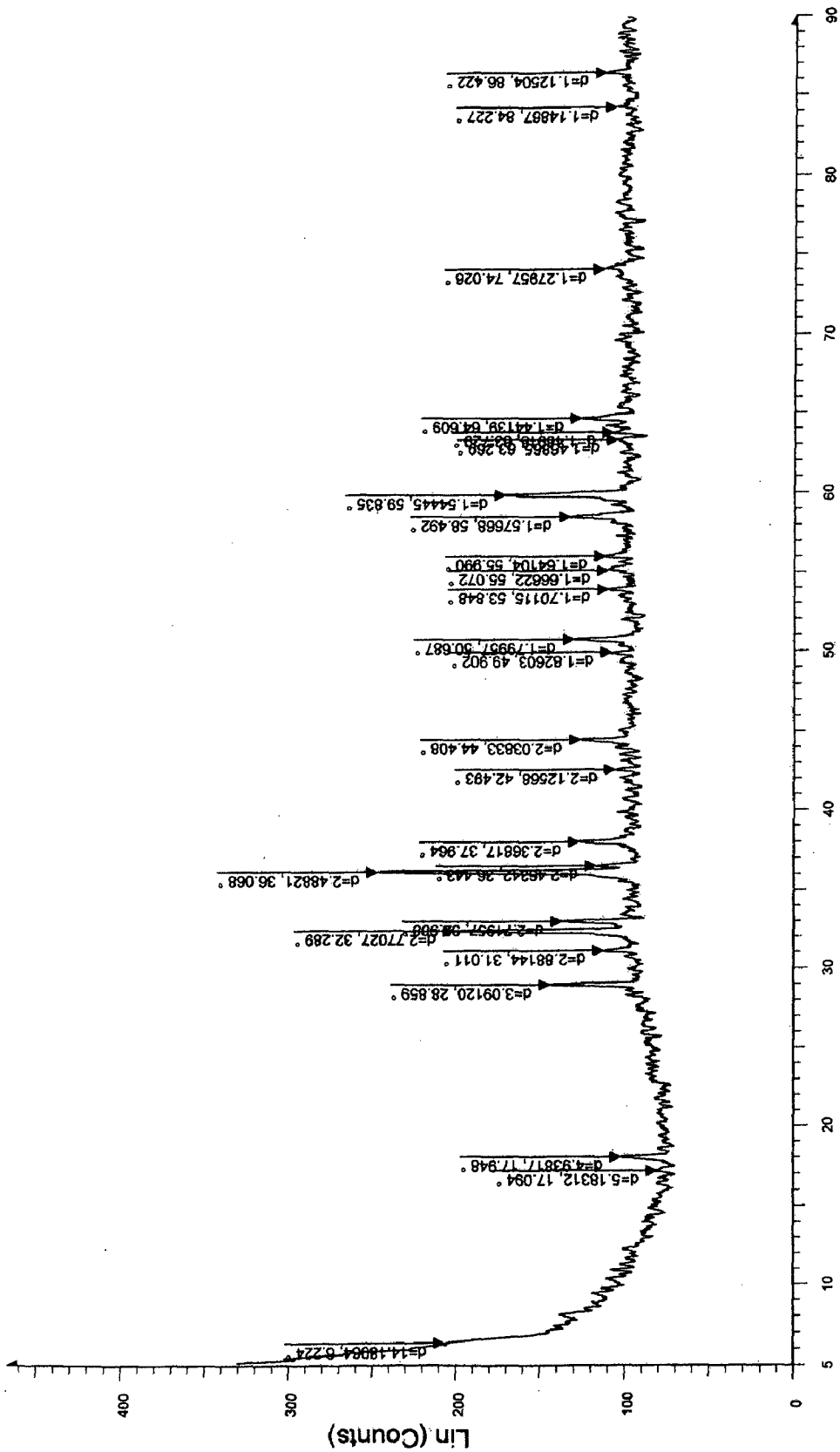


Fig. 6 XRD graph for Manganese oxide at 650°C temperature in presence of air.



JM-1000 - File: M-1000.raw - Type: 2Th/Th-locked - Start: 5.000 ° - End: 80.006 ° - Step: 0.019 ° - Temp.: 25 °C (Room) - Time Started: 12 s - 2-Theta: 5.000 ° - Theta: 2.500 ° -
 Operations: Smooth 0.150 | Y Scale Mul 0.750 | Import

Fig. 7 XRD graph for Manganese oxide at 1000°C temperature in presence of air.

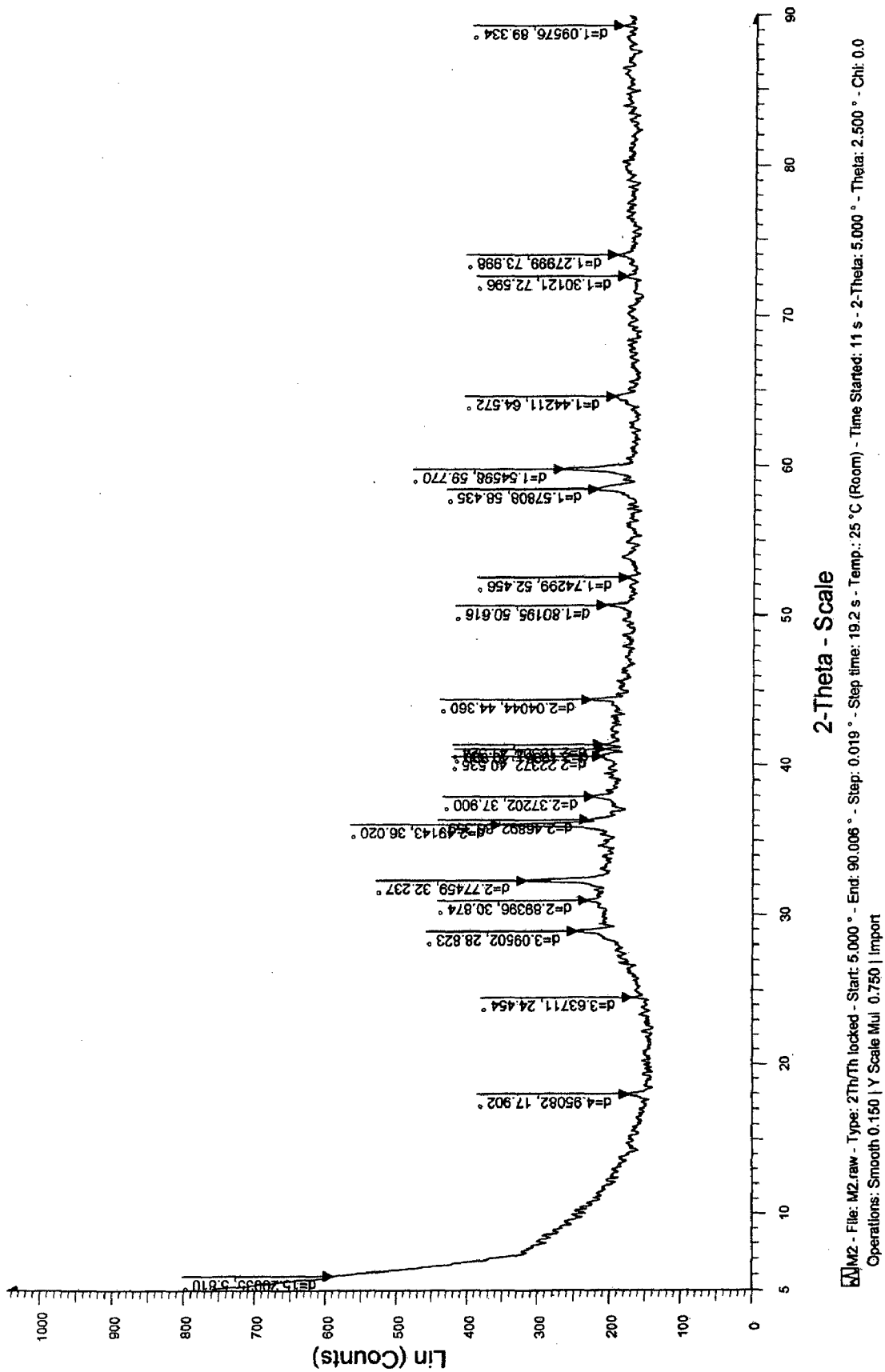


Fig. 9 XRD graph for Manganese oxide at 650°C temperature in Argon environment.

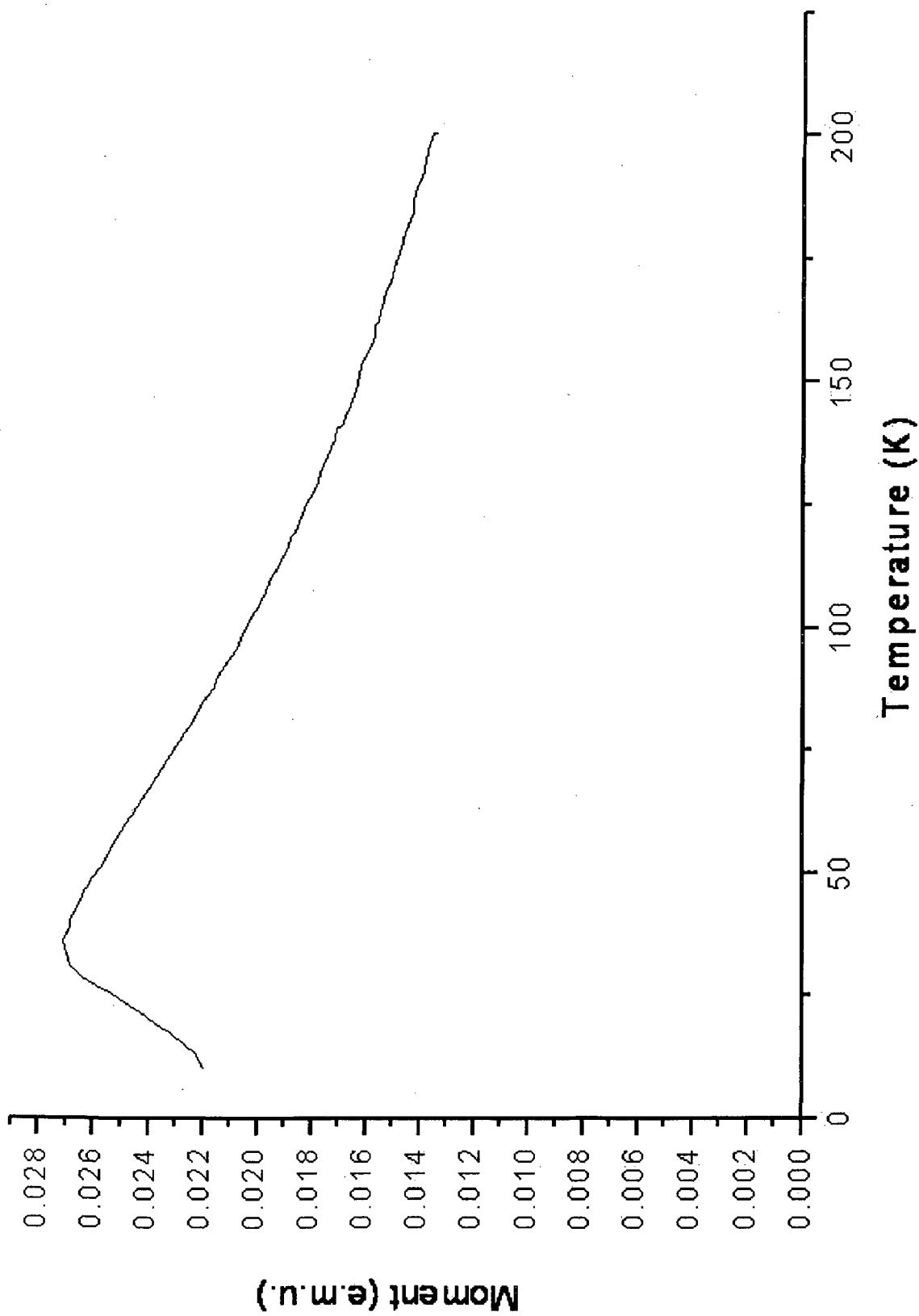


Fig. 10 Magnetization graph of Mn_3O_4 at $450^\circ C$ temperature in nitrogen environment

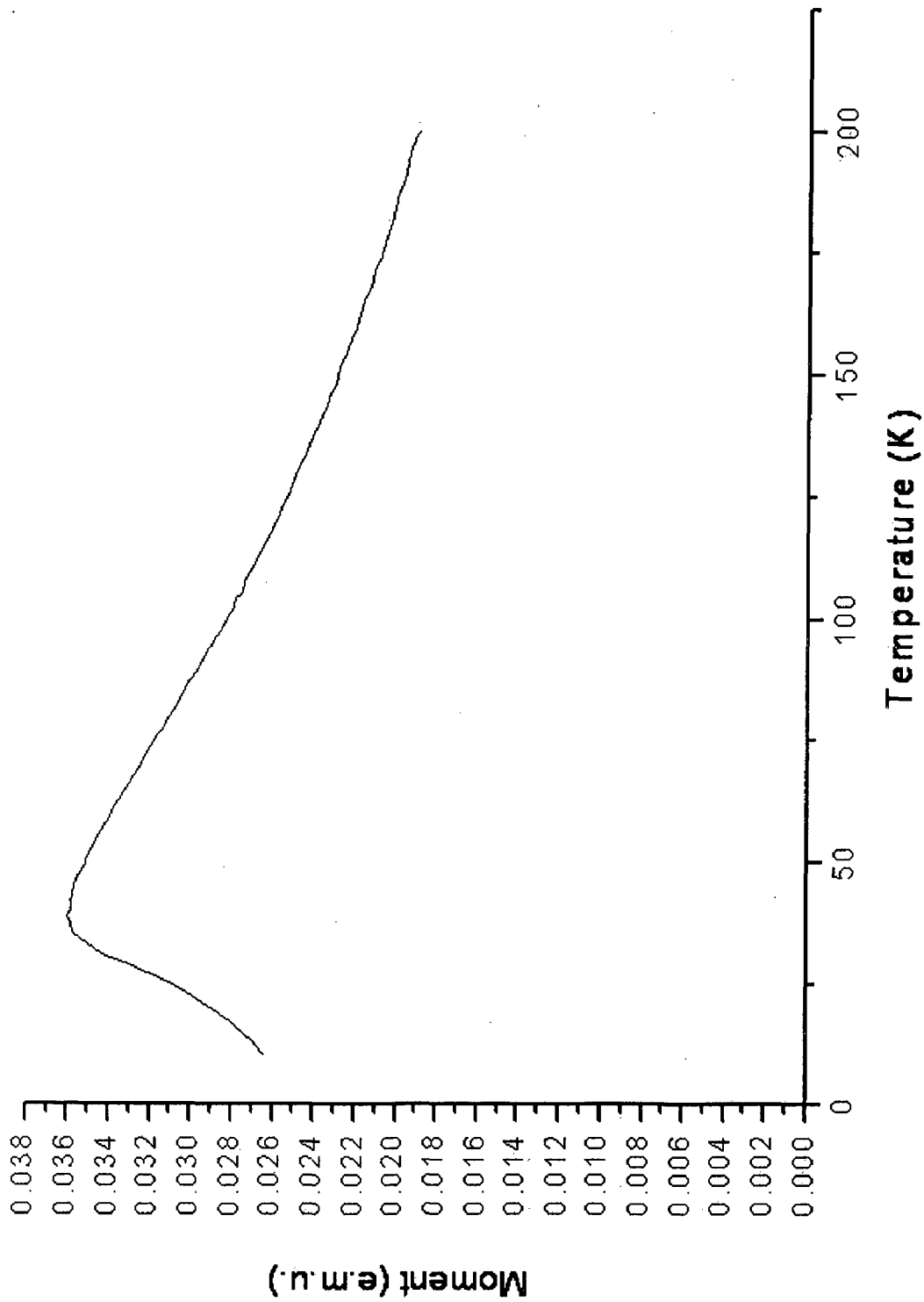


Fig. 11 Magnetization graph of Mn₃O₄ at 650°C temperature in Argon environment

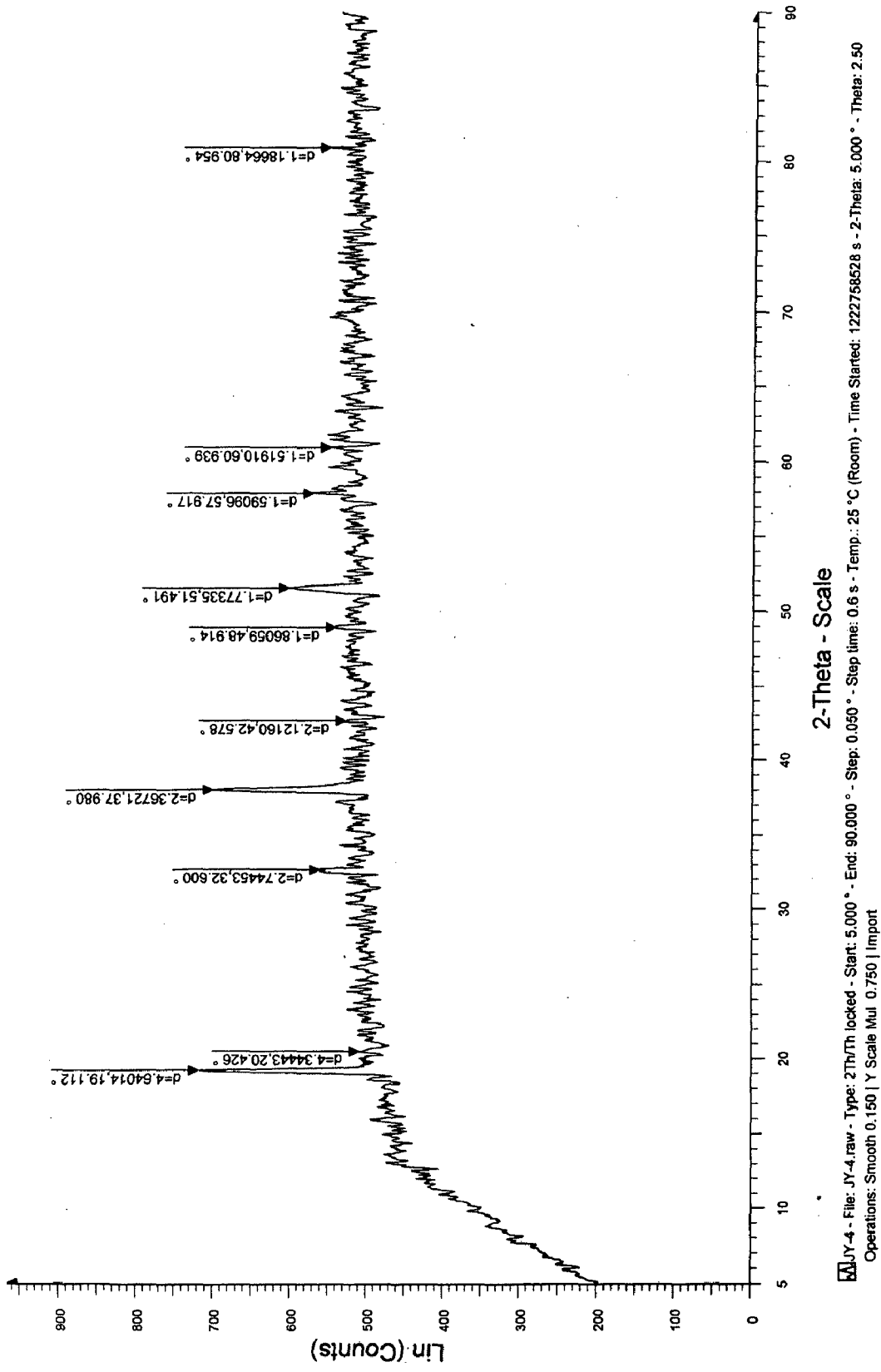


Fig. 12 XRD graph for Cobalt oxide precursor at room temperature.

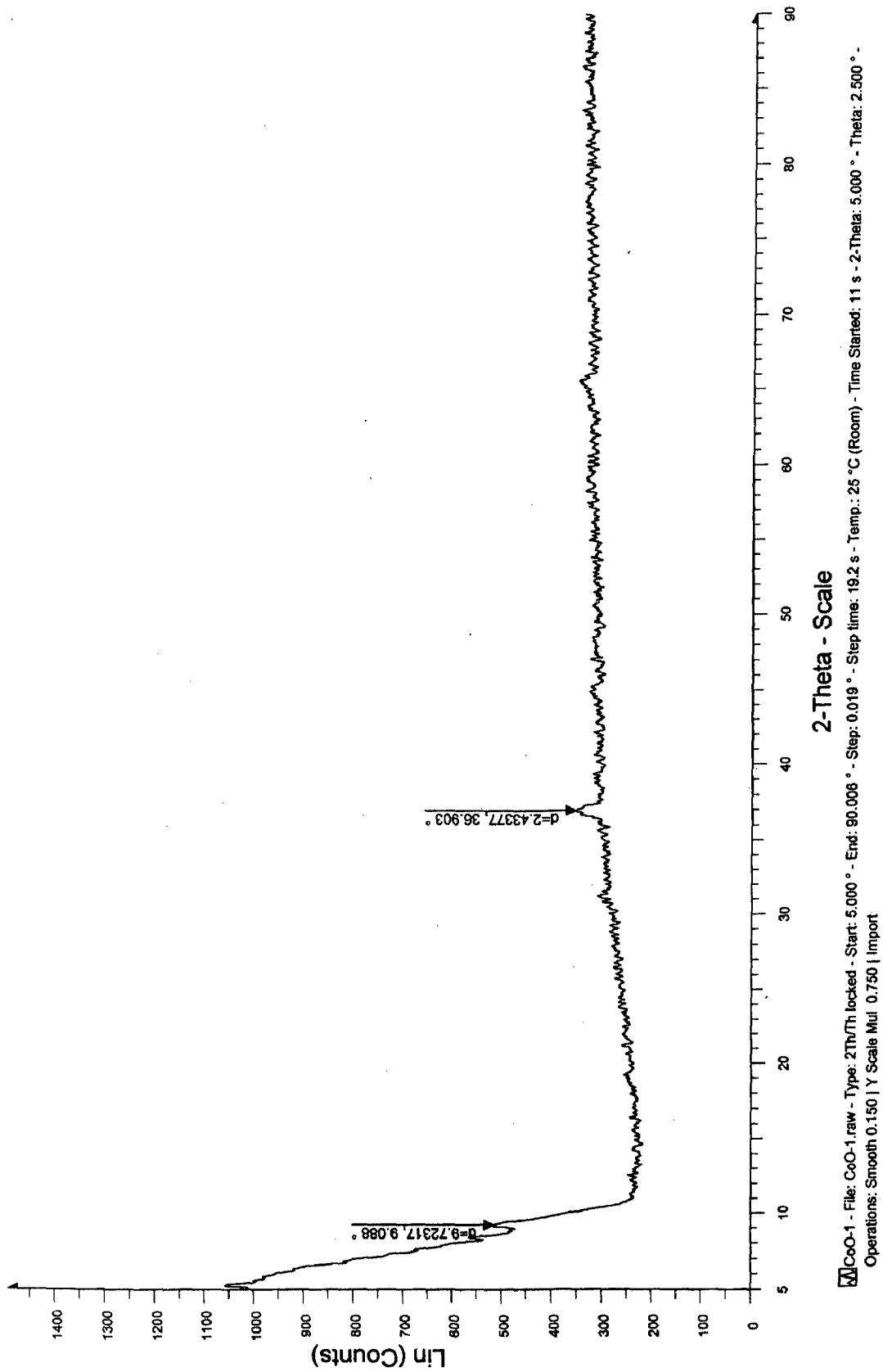


Fig. 13 XRD graph for Cobalt oxide precursor at 200°C temperature in presence of air.

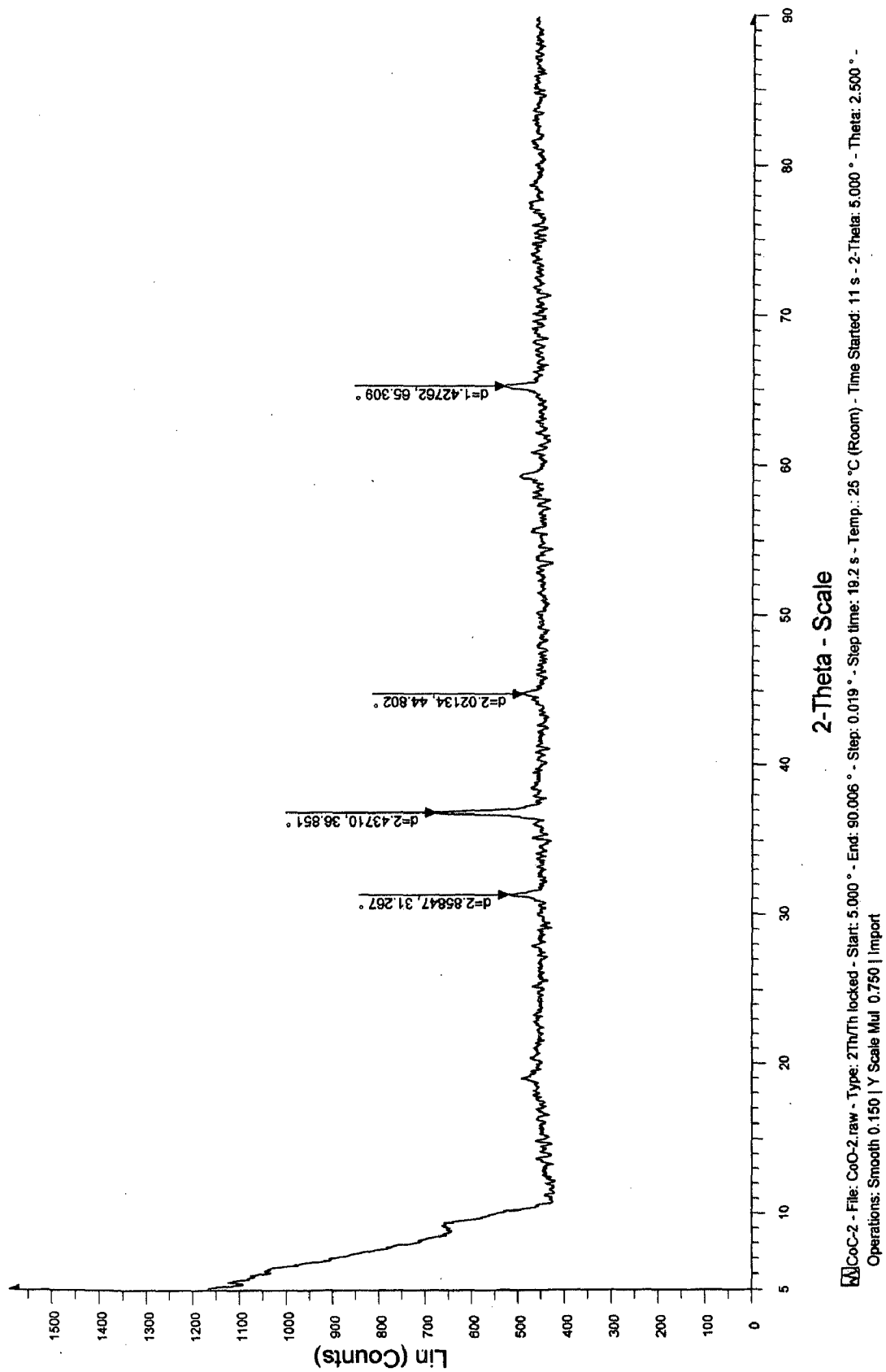
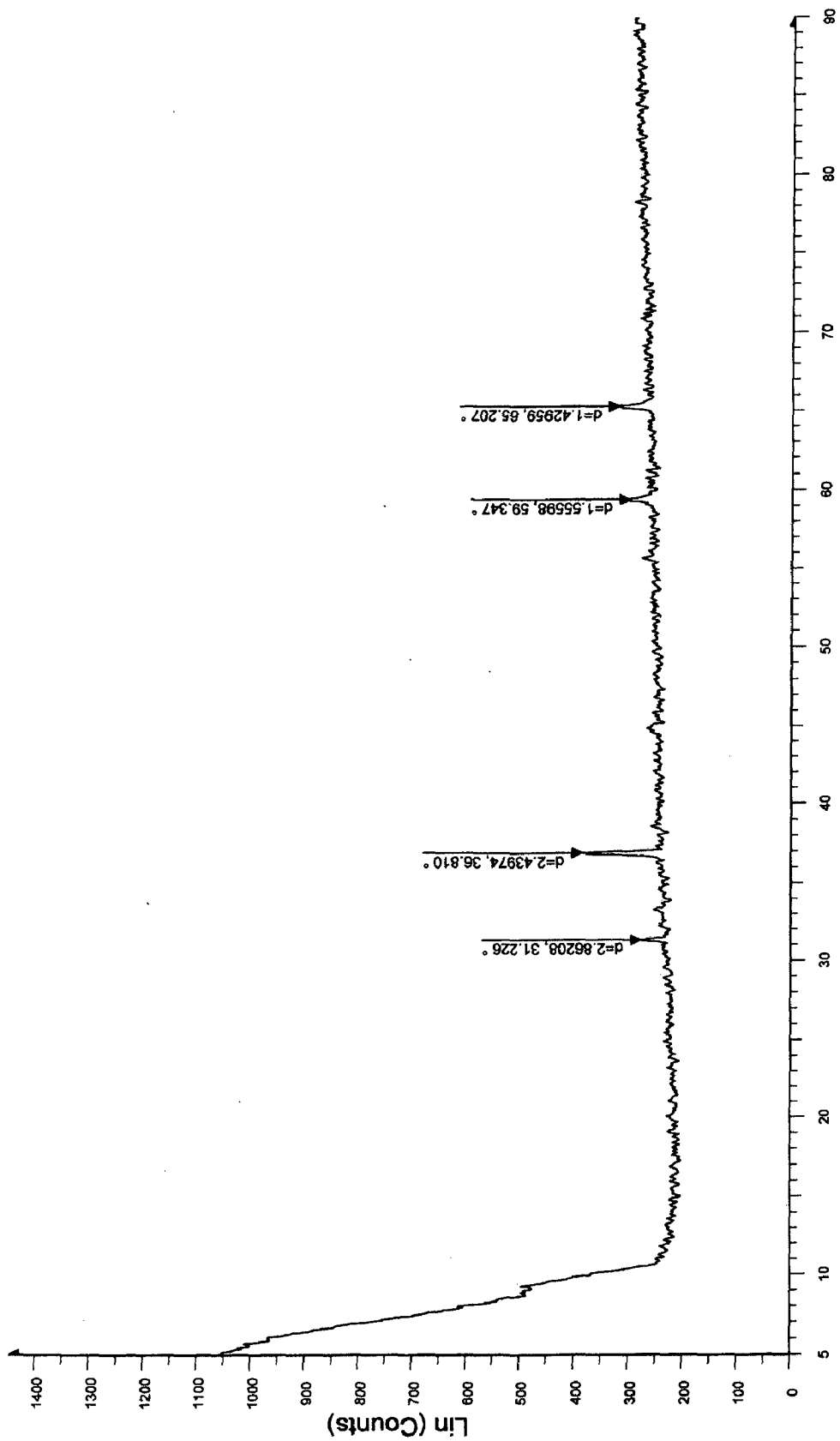


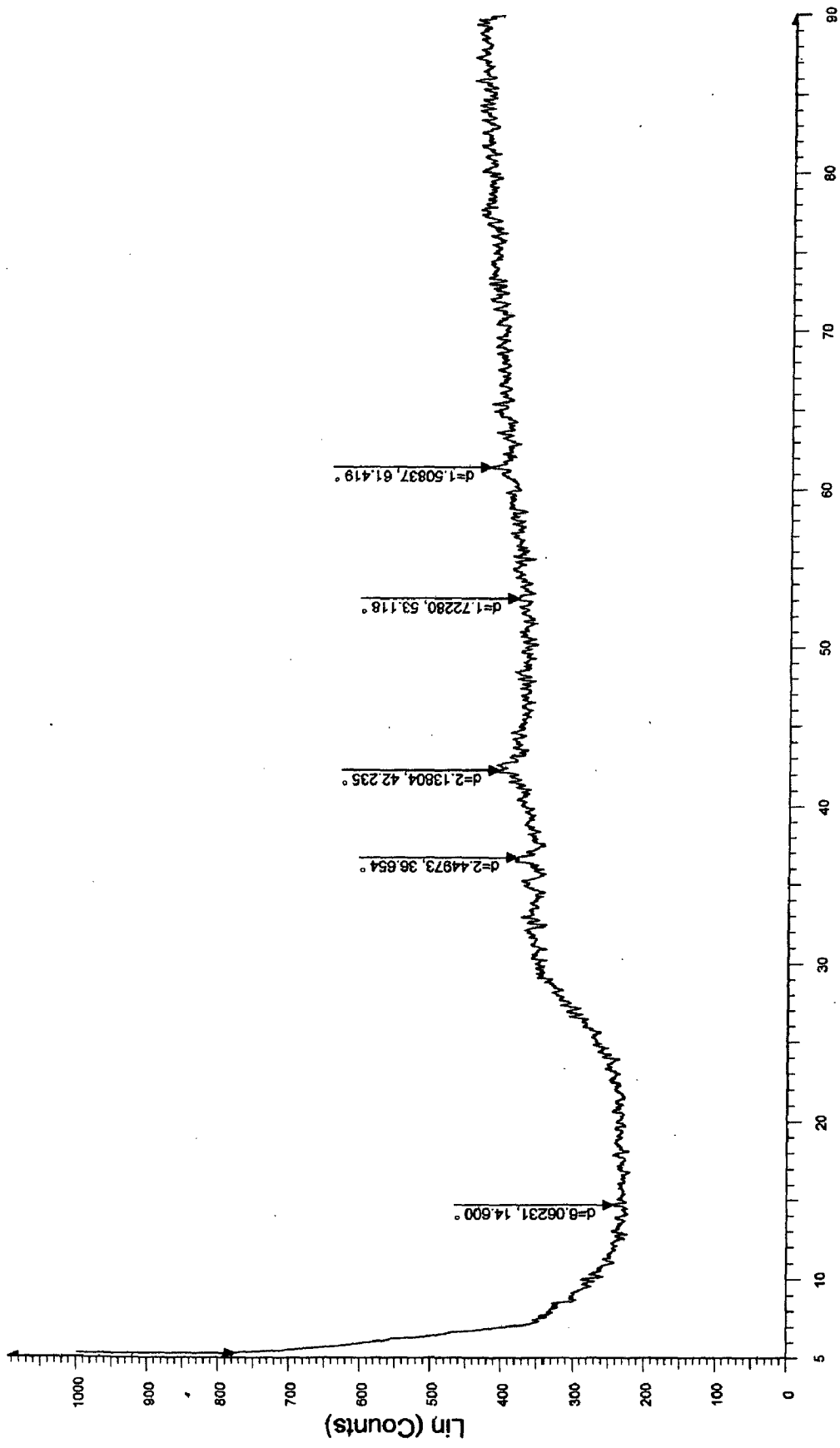
Fig. 14 XRD graph for Cobalt oxide precursor at 450°C temperature in presence of air.



2-Theta - Scale

CoO-3 - File: CoO-3.raw - Type: 2Th/Th locked - Start: 5.000 ° - End: 90.006 ° - Step: 0.019 ° - Step time: 19.2 s - Temp.: 25 °C (Room) - Time Started: 12 s - 2-Theta: 5.000 ° - Theta: 2.500 ° - Operations: Smooth 0.150 | Y Scale Mul 0.750 | Import

Fig. 15 XRD graph for Cobalt oxide precursor at 950°C temperature in presence of air.



C1 - File: C1.raw - Type: 2Th/Th locked - Start: 5.000 ° - End: 90.006 ° - Step: 0.019 ° - Step time: 19.2 s - Temp.: 25 °C (Room) - Time Started: 11 s - 2-Theta: 5.000 ° - Theta: 2.500 ° - Chi: 0.0
 Operations: Smooth 0.150 | Y Scale Mul 0.750 | Import

Fig. 16 XRD graph for Cobalt oxide precursor at 450°C temperature in presence of nitrogen.

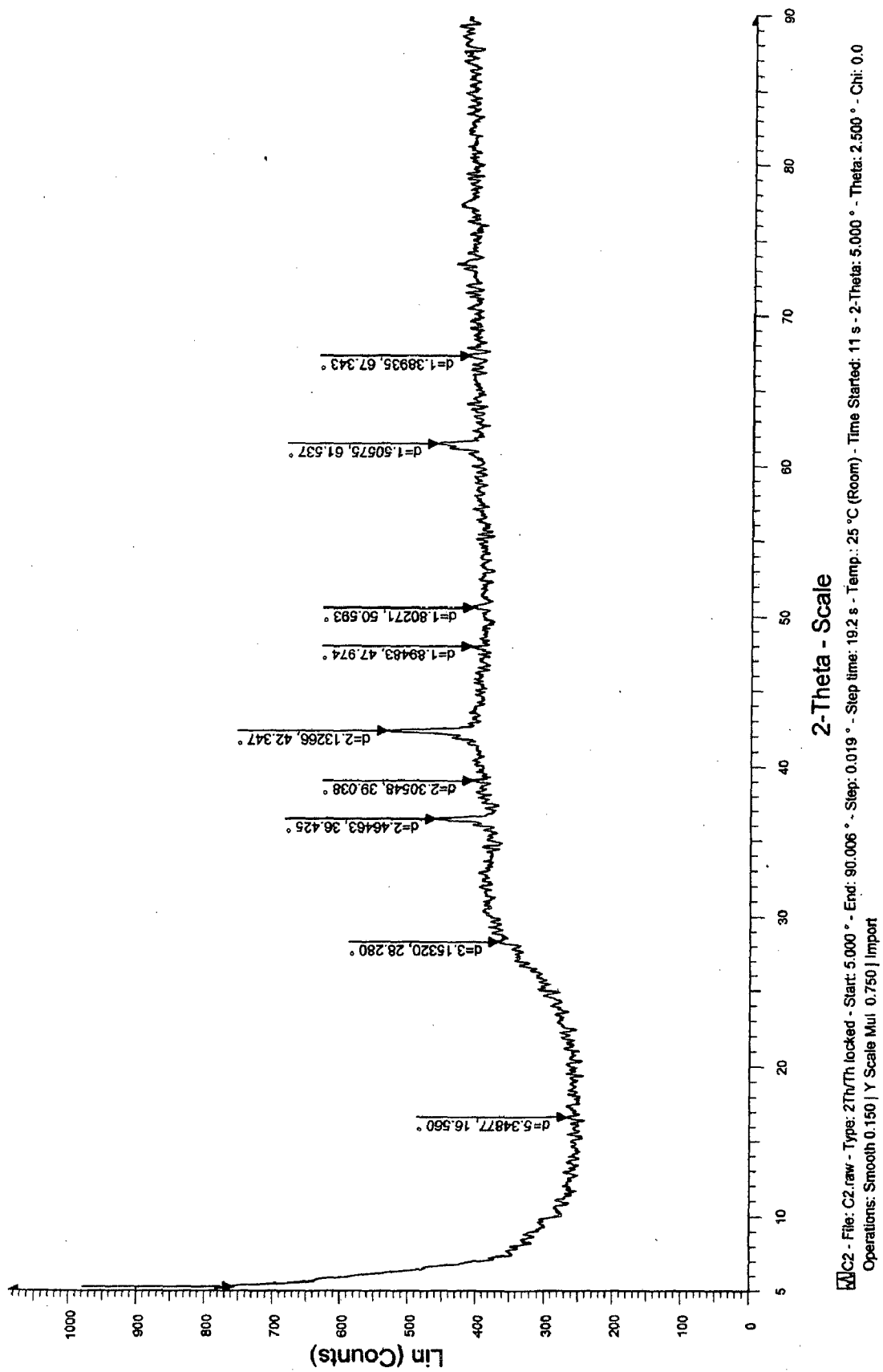
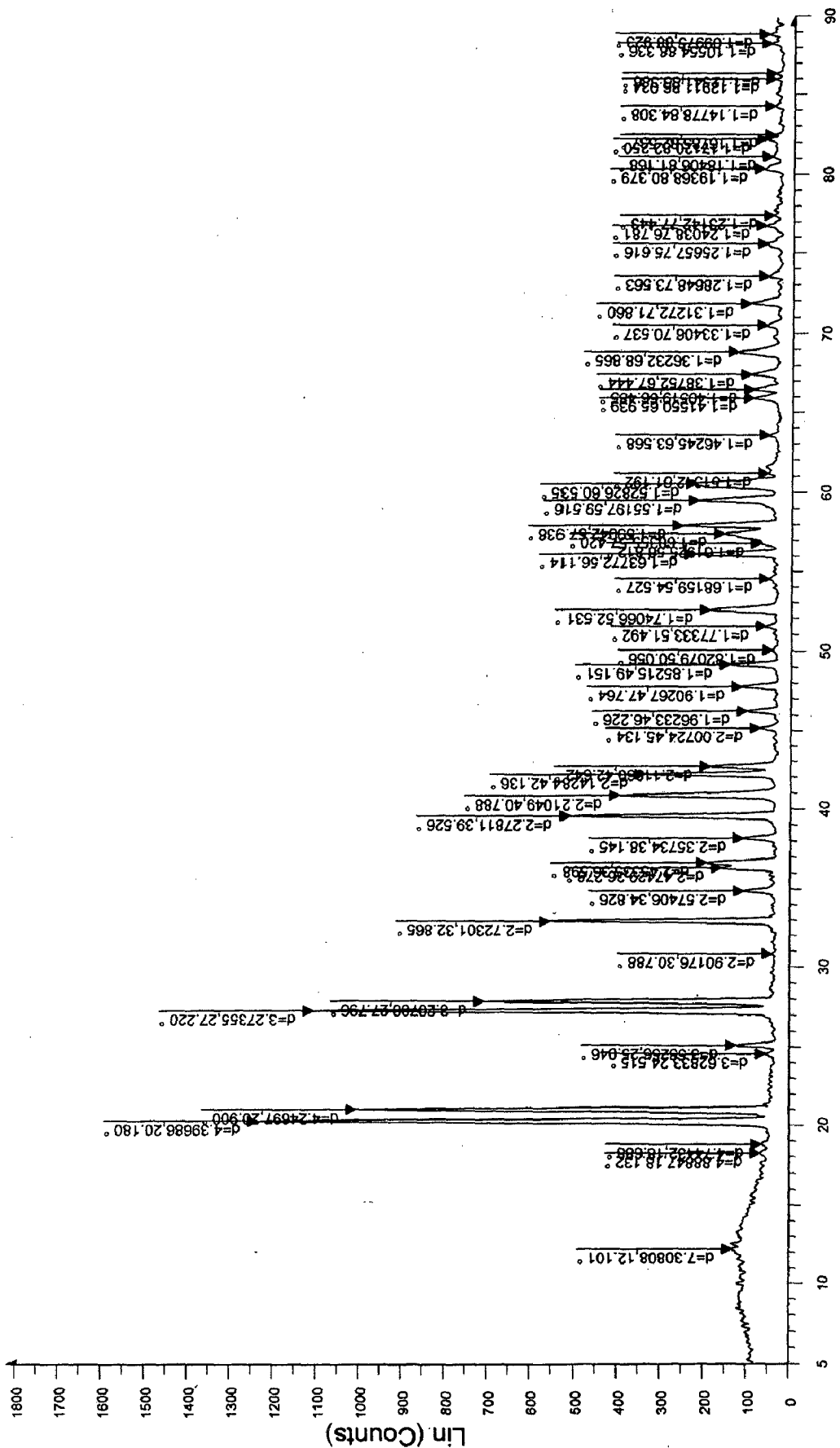


Fig.17 XRD graph for Cobalt oxide precursor at 450°C temperature in presence of Argon.



JY-1 - File: JY-1.raw - Type: 2Th/Th locked - Start: 5.000 ° - End: 90.000 ° - Step: 0.050 ° - Step time: 0.6 s - Temp.: 25 °C (Room) - Time Started: 1222787872 s - 2-Theta: 5.000 ° - Theta: 2.50
 Operations: Smooth 0.150 | Y Scale Mul 0.750 | Import

Fig. 18 XRD graph for Zinc oxide precursor.

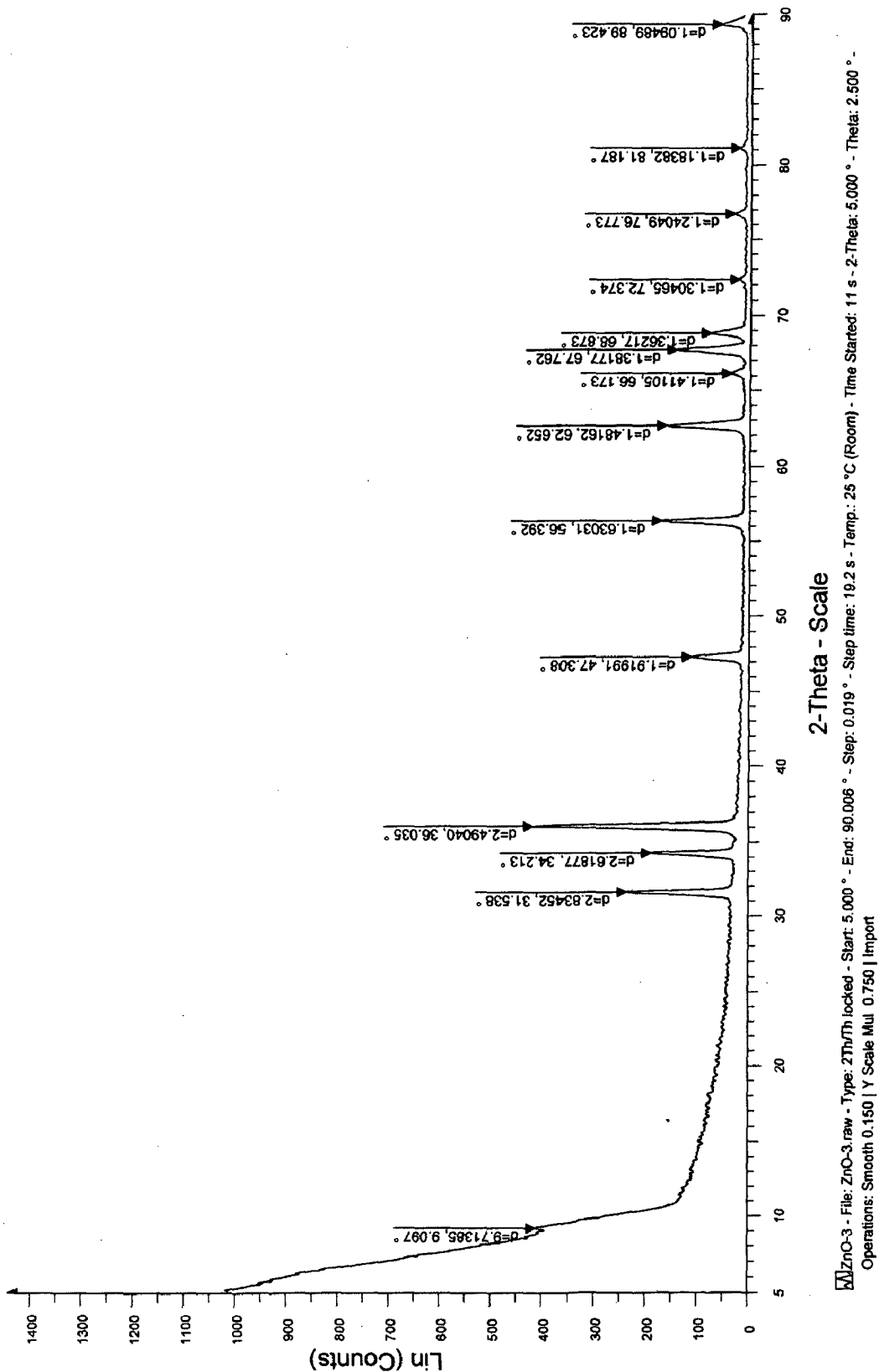
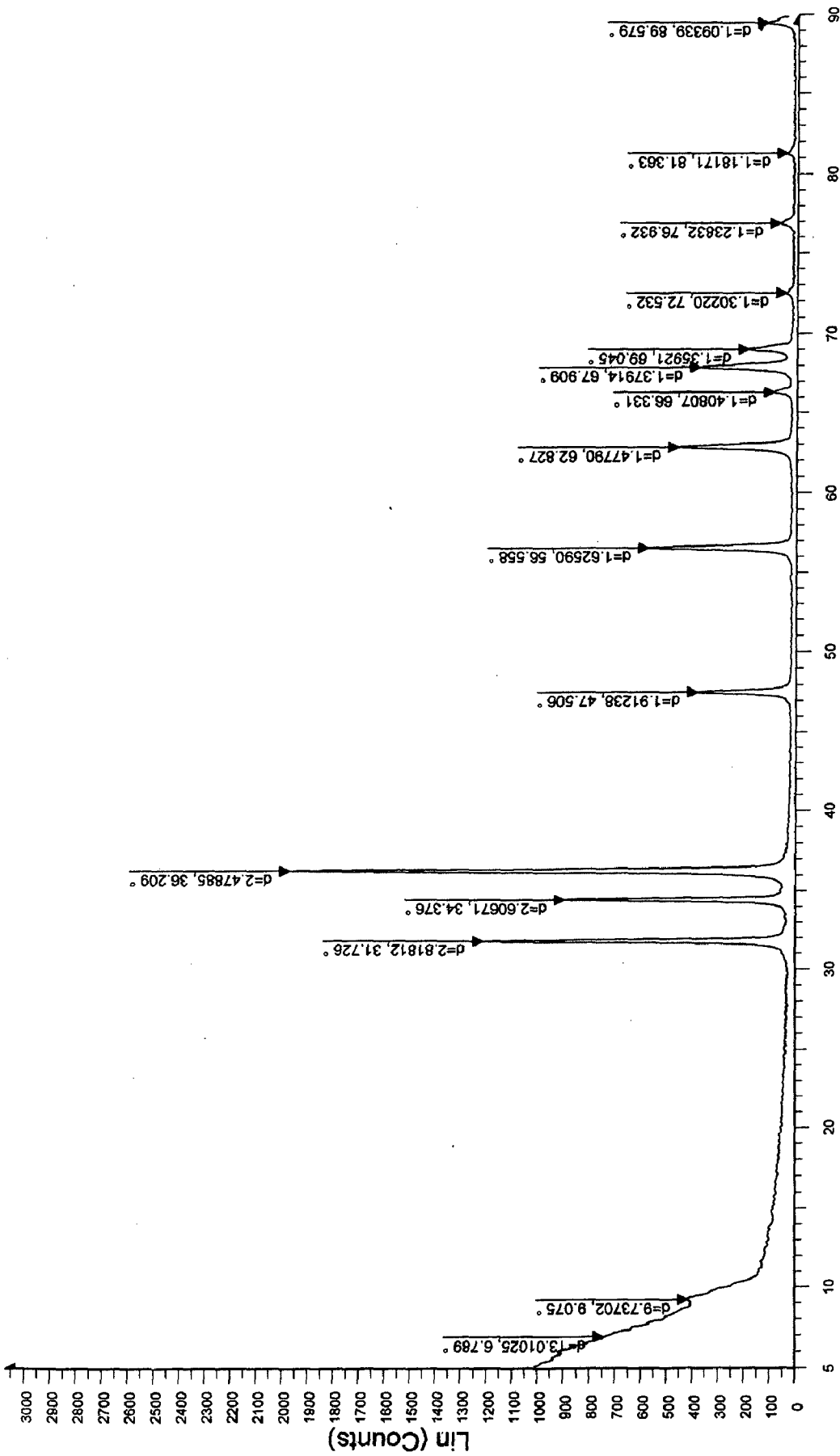


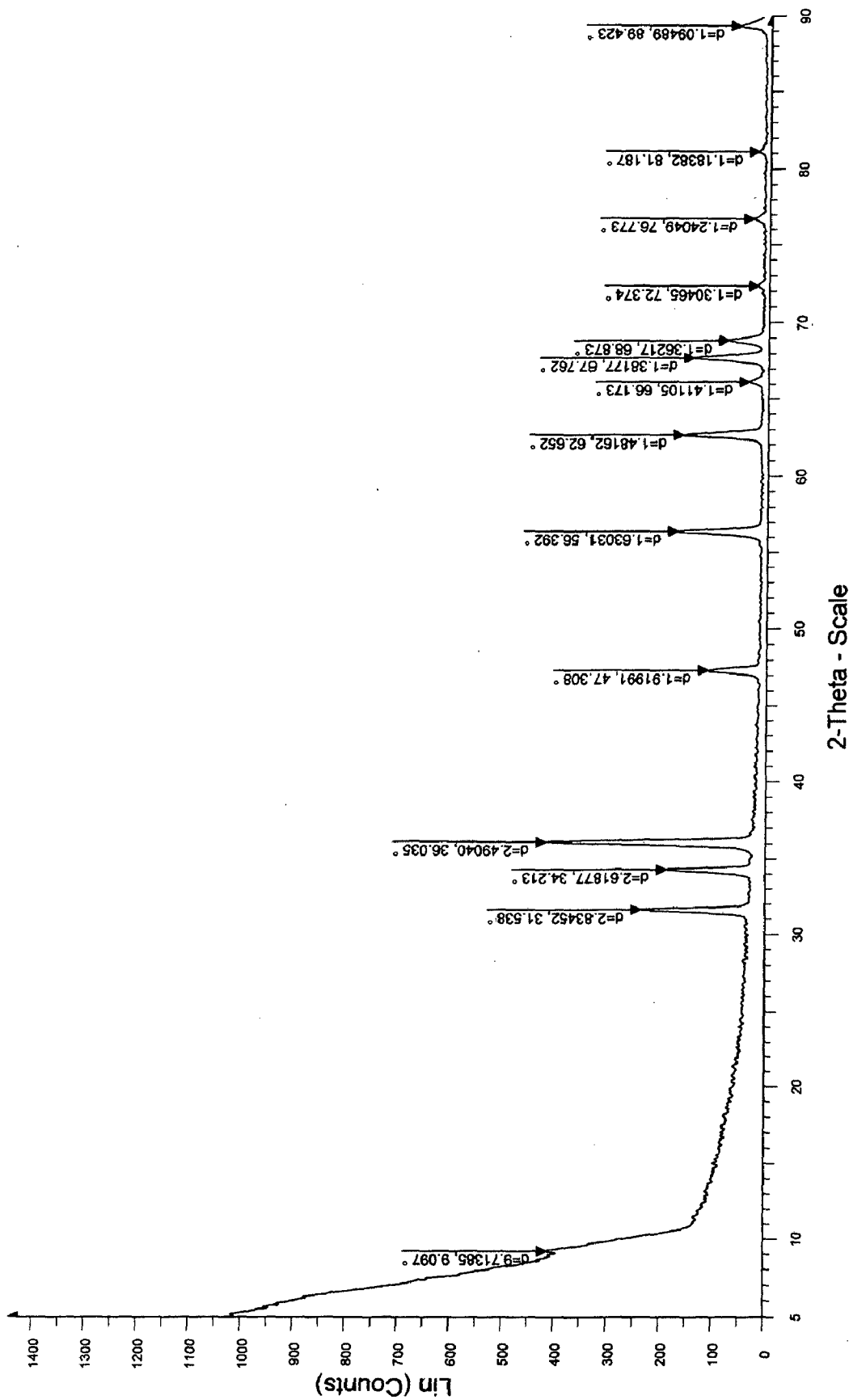
Fig.19 XRD graph for Zinc oxide at 200°C in presence of air.



2-Theta - Scale

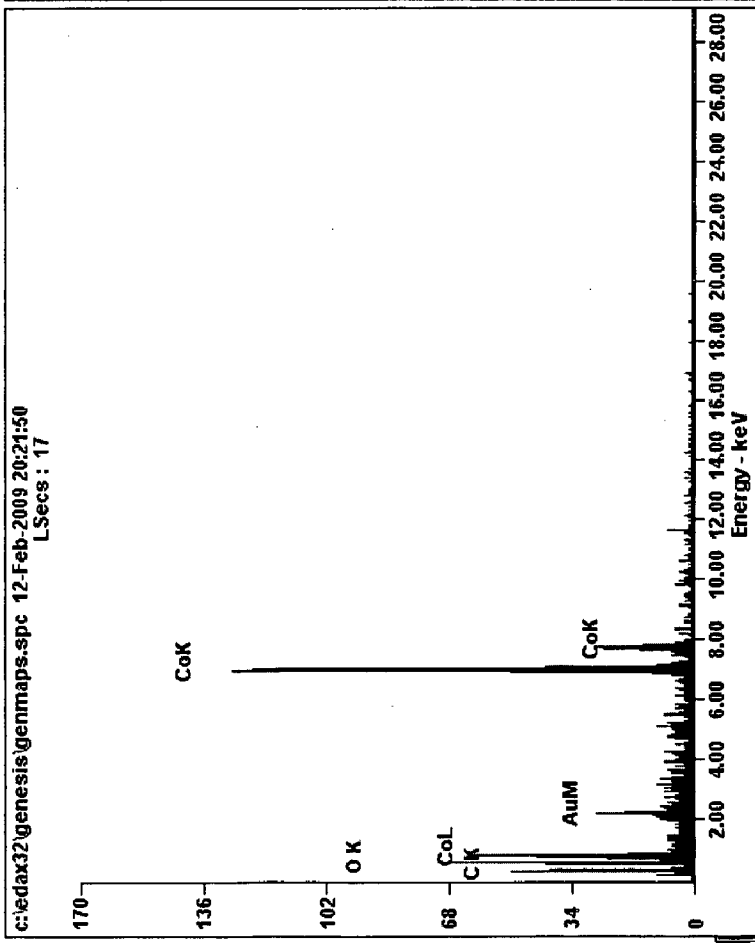
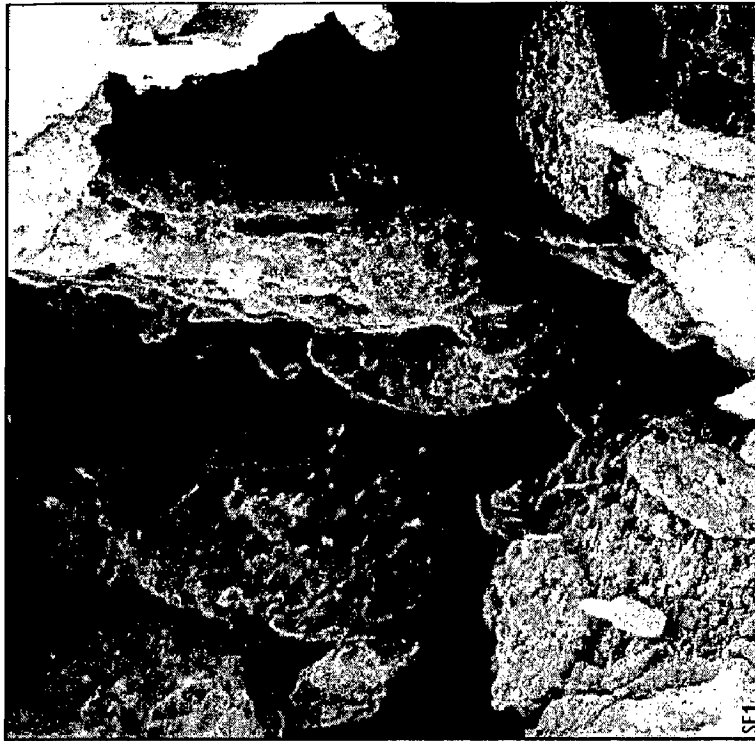
ZnO-2 - File: ZnO-2.raw - Type: 2Th/Th locked - Start: 5.000 ° - End: 90.006 ° - Step: 0.019 ° - Step time: 19.2 s - Temp.: 25 °C (Room) - Time Started: 11 s - 2-Theta: 5.000 ° - Theta: 2.500 ° - Operations: Smooth 0.150 | Y Scale Mul 0.750 | Import

Fig.20 XRD graph for Zinc oxide at 450°C in presence of air.



ZnO-3 - File: ZnO-3.raw - Type: 2ThTh locked - Start: 5.000° - End: 90.006° - Step: 0.019° - Temp.: 25 °C (Room) - Time Started: 11 s - 2-Theta: 5.000° - Theta: 2.500°
 Operations: Smooth 0.150 | Y Scale Mult 0.750 | Import

Fig.21 XRD graph for Zinc oxide at 950°C in presence of air

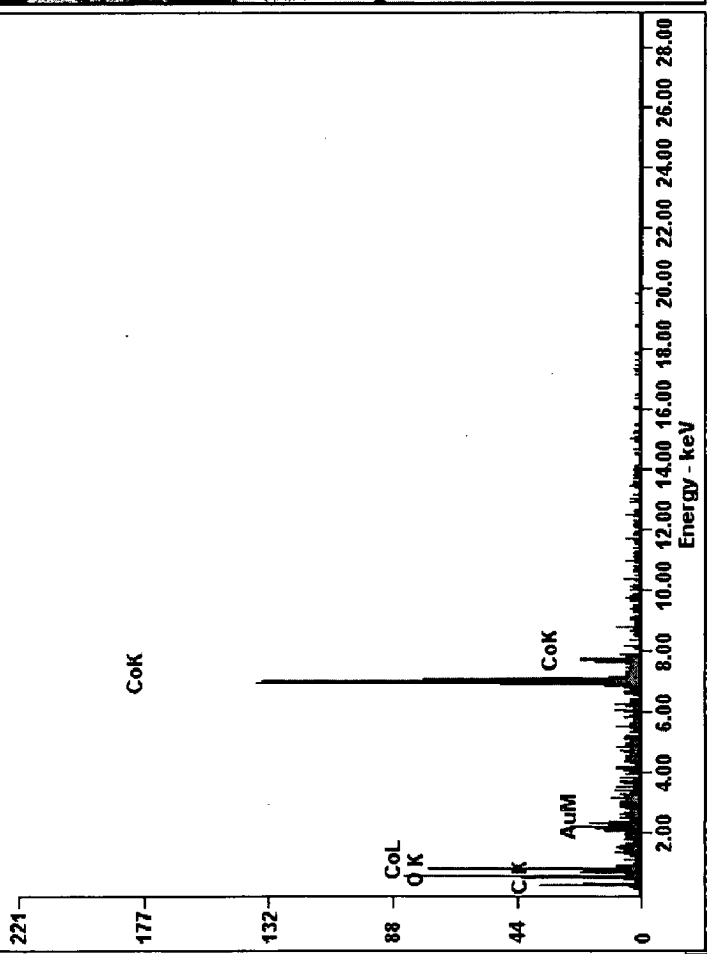


c:\edax32\genesis\genmaps.spc 12-Feb-2009 20:21:50
LSecs : 17

<i>CK</i>	26.31	53.93
<i>OK</i>	15.27	23.49
<i>AuM</i>	06.22	00.78
<i>CoK</i>	52.19	21.80
<i>Matrix</i>	Correction	ZAF

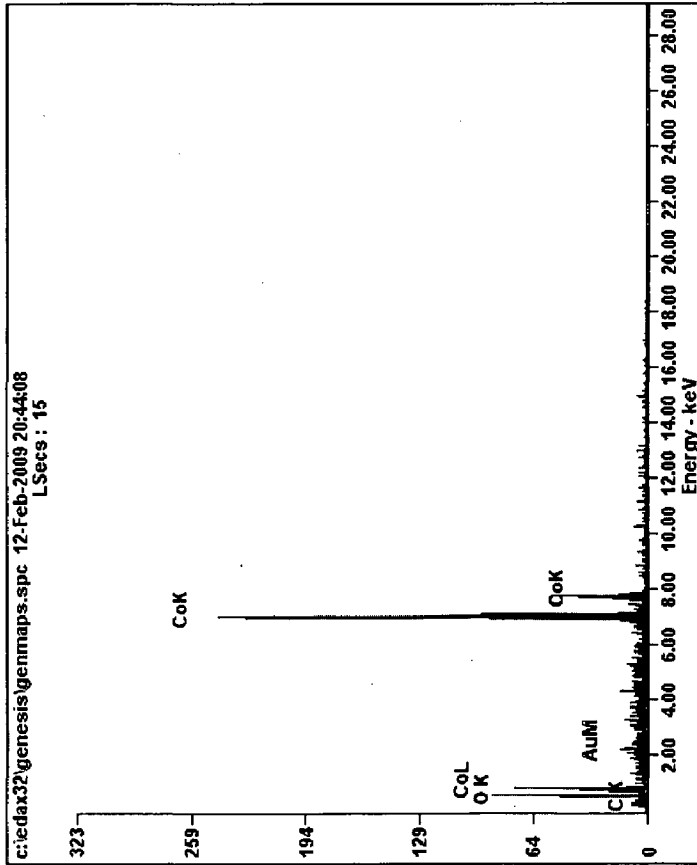
Fig. 22 SEM image & EDAX data of cobalt oxide at 200°C in presence of air.

c:\edax32\genesis\genmaps.spc 12-Feb-2009 20:35:45
LSecs : 16



Element	WT%	AT%
<i>CK</i>	17.19	42.01
<i>OK</i>	13.99	25.66
<i>AuM</i>	05.59	00.83
<i>CoK</i>	63.23	31.49
<i>Matrix</i>	Correction	ZAF

Fig. 23 SEM image & EDAX data of cobalt oxide at 450°C in presence of air.



Element	WT%	AT%
CK	01.95	07.18
OK	10.64	29.42
AuM	04.21	00.95
CoK	83.20	62.45
Matrix	Correction	ZAF

Fig. 24 SEM image & EDAX data of cobalt oxide at 950°C in air.

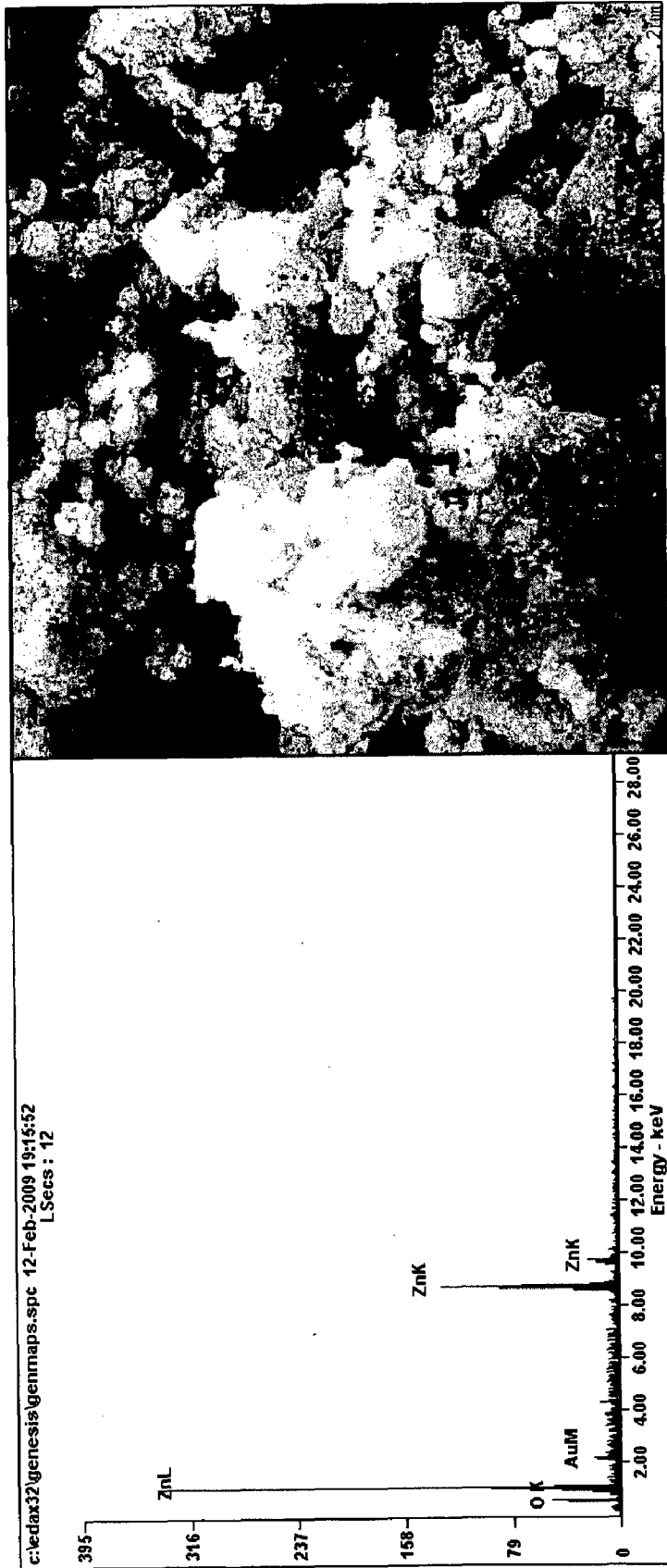
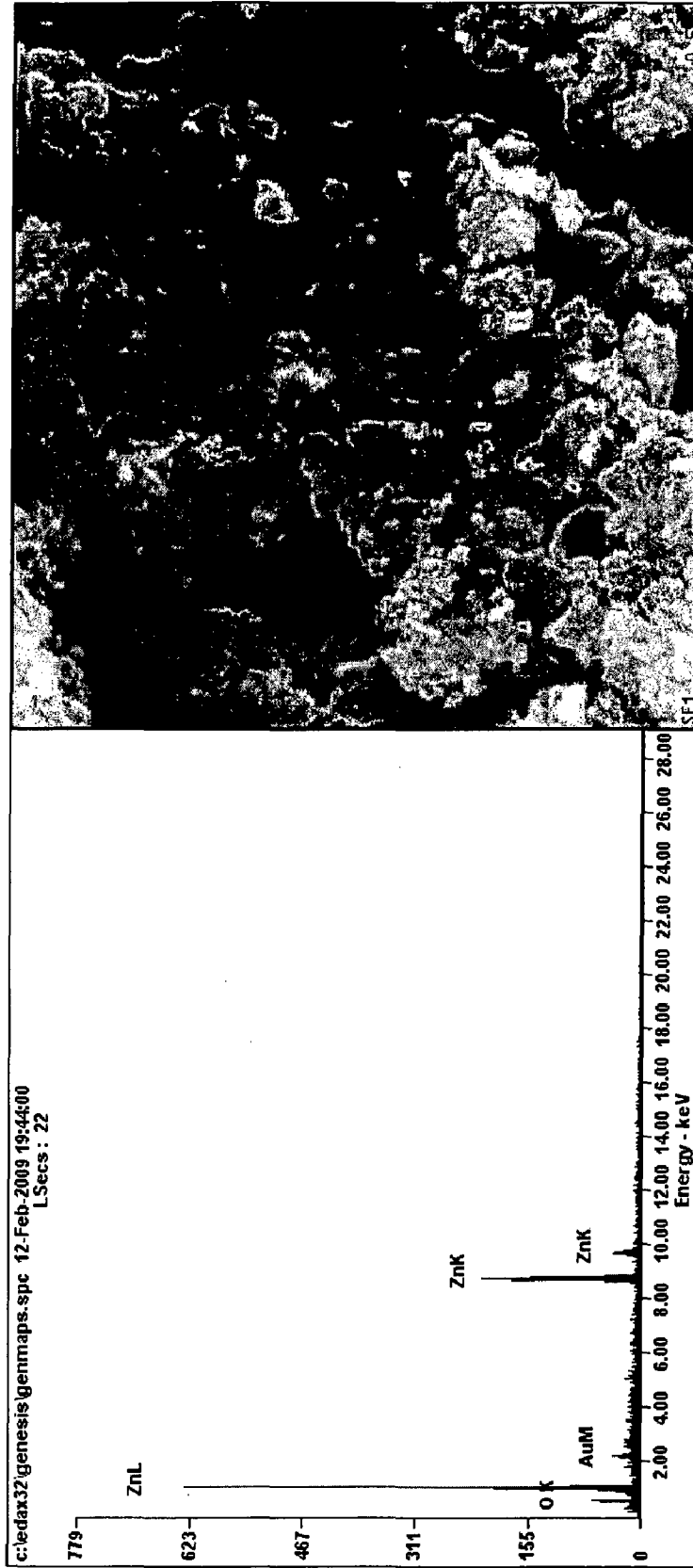


Fig. 25 SEM image & EDAX data of zinc oxide at 200⁰C in air.

Element	Wt%	At%
OK	08.80	28.97
AuM	04.55	01.22
ZnK	86.65	69.82
Matrix	Correction	ZAF



Element	Wt%	At%
<i>OK</i>	07.62	26.18
<i>AuM</i>	06.79	01.89
<i>ZnK</i>	85.59	71.93
<i>Matrix</i>	Correction	ZAF

Fig. 26 SEM image & EDAX data of zinc oxide at 450°C in air

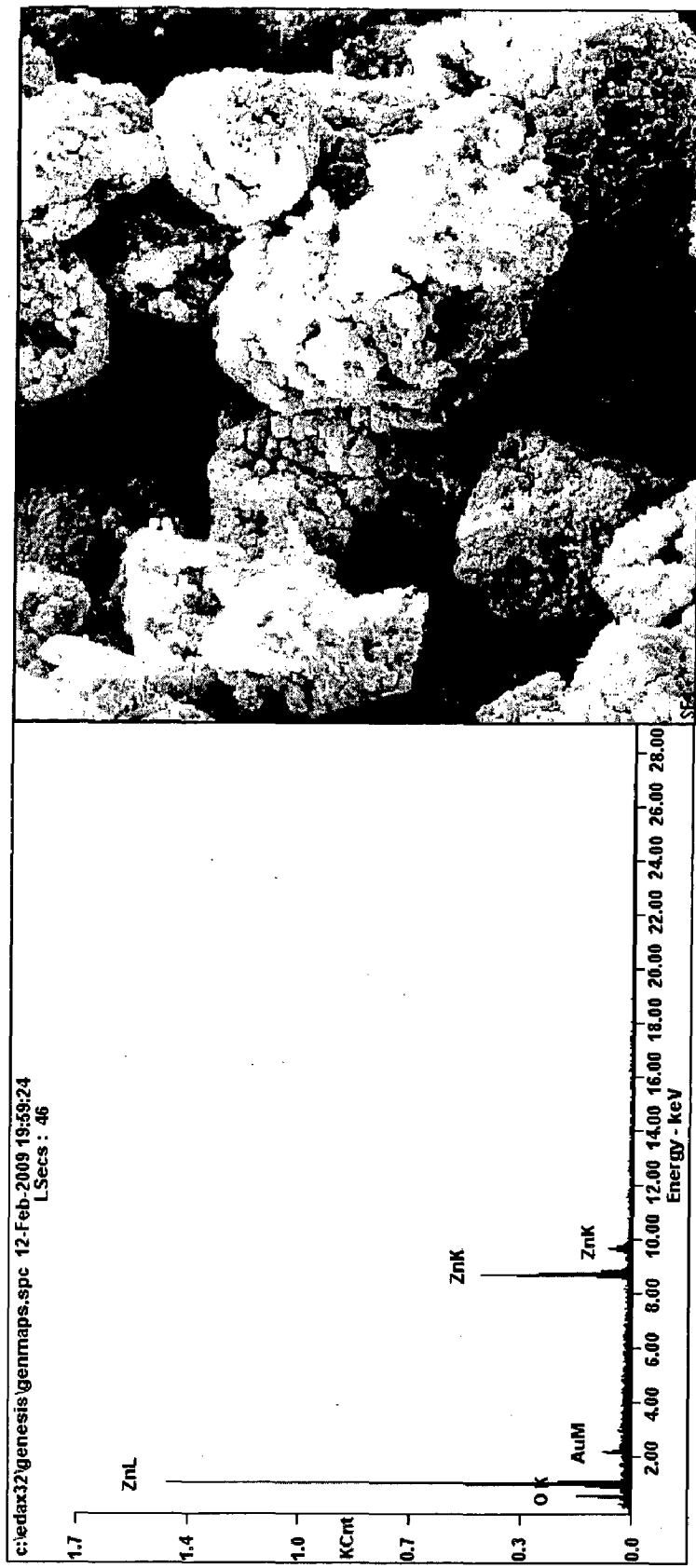


Fig. 27 SEM image & EDAX data of zinc oxide at 950°C in air

Element	Wt%	At%
<i>OK</i>	08.80	29.11
<i>AuM</i>	05.46	01.47
<i>ZnK</i>	85.74	69.43
<i>Matrix</i>	Correction	ZAF